JAAS

ROYAL SOCIETY OF CHEMISTRY

CRITICAL REVIEW

Published on 04 August 2026

Cite this: DOI: 10.1039/d6ja00223d

Laser-induced breakdown spectroscopy for phosphorus analysis: current challenges and critical perspectives

Stefano Legnaioli,[a] Giulia Lorenzetti,[a] Francesco Poggialini,[a] Beatrice Campanella,[a] Vincenzo Palleschi,*[a] Giorgio Saverio Senesi,[b] Silvana De Iuliis,[c] Laura Eleonora Depero,[d] Laura Borgese[d] and Elza Bontempi[d]

Phosphorus is essential for global food security as an irreplaceable component of fertilizers, and it also finds widespread application across numerous industrial and technological fields. Because of its critical role and the significant risk of supply shortages, the European Commission has designated phosphorus as a critical raw material. Consequently, there is a growing need for fast, robust, and adaptable analytical techniques capable of accurately determining phosphorus in environmental, agricultural, industrial, and recycling contexts. Among these, Laser-Induced Breakdown Spectroscopy (LIBS) has gained prominence, offering multi-element capability, minimal sample preparation requirements, and the ability to perform *in situ* and real-time analyses. This review provides a comprehensive overview of the experimental methodologies and analytical strategies for LIBS-based phosphorus quantification across a wide range of matrices, including soils, rocks, fertilizers, biological samples, industrial materials, and secondary resources. Particular emphasis is placed on the current challenges associated with phosphorus analysis by LIBS, including matrix effects, calibration transferability, and the reliability of advanced chemometric and machine-learning approaches. The review also discusses recent progress in calibration methods, signal-enhancement techniques, handheld instrumentation, and strategies aimed at improving analytical robustness and reducing matrix-related effects. By critically assessing both recent advances and persisting limitations, the review highlights the growing relevance of LIBS as a powerful analytical tool for sustainable phosphorus management and the development of circular-economy initiatives, while also providing critical perspectives on the future evolution of the technique for reliable phosphorus quantification.

Received 4th June 2026
Accepted 27th July 2026

DOI: 10.1039/d6ja00223d

rsc.li/jaas

1. Introduction

Phosphorus and its compounds play a central role in numerous scientific, technological, and socio-economic fields, representing a strategic resource for the sustainable development of our society.[1,2] Fig. 1 schematically represents the major fields in which phosphorus is used, with the relevant approximate percentages.

In the industrial sector, phosphorus is used in the production of metal alloys, additives for polymeric materials,

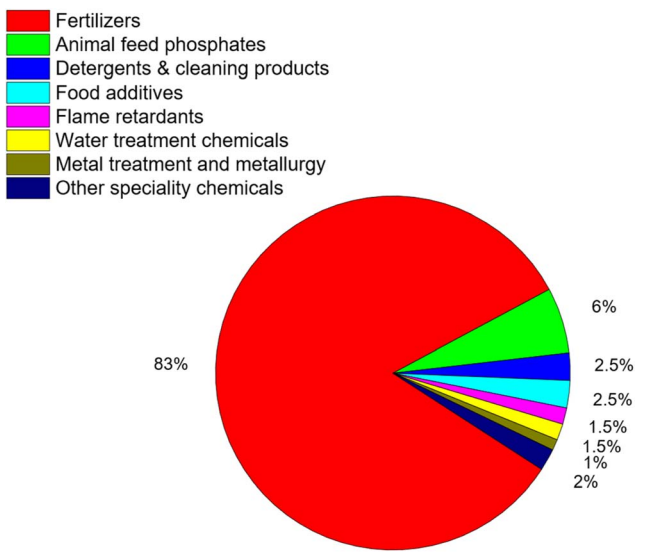

Fig. 1 Main applications of phosphorus in agriculture and industry. Approximate distribution based on USGS Mineral Commodity Summaries (2025)[2] and International Fertilizer Association statistics.[3]

[a]*Institute of Chemistry of Organometallic Compounds, National Research Council, 56124 Pisa, Italy. E-mail: stefano.legnaioli@cnr.it; giulia.lorenzetti@cnr.it; francesco.poggialini@cnr.it; beatrice.campanella@cnr.it; vincenzo.palleschi@cnr.it*

[b]*Institute for Plasma Science and Technology (ISTP), National Research Council, Bari, Italy. E-mail: giorgio.senesi@cnr.it*

[c]*Institute of Condensed Matter Chemistry and Energy Technologies, National Research Council, 20125 Milano, Italy. E-mail: silvana.deiuliis@cnr.it*

[d]*INSTM, Chemistry for Technologies Laboratory, Department of Mechanical and Industrial Engineering, University of Brescia, 25121 Brescia, Italy. E-mail: laura.depero@unibs.it; laura.borgese@unibs.it; elza.bontempi@unibs.it*

detergents, flame retardants, and numerous chemical processes, where phosphates and other phosphorus derivatives help to improve the performance of the final products by enhancing properties such as flame resistance, corrosion protection, thermal stability, wear resistance, catalytic activity, buffering capacity, and metal surface passivation.[4]

In the agricultural sector, phosphorus is of primary importance: together with nitrogen and potassium, it is one of the essential macronutrients for plant growth and is therefore a key component of mineral fertilizers. The availability and rational use of phosphorus are closely linked to global food security, while an excess of phosphorus can cause significant environmental problems, such as eutrophication of surface waters.[3,5,6]

The size of the phosphorus and derivatives market is estimated at 70 billion USD in 2024 and is expected to reach 100 billion USD by 2032.[7]

From the point of view of the resources, it is expected that the deposits of phosphate rock currently available would cover the world's needs for about one century.[1,2] Despite that, the European Commission has included phosphate rock in the list of Critical Raw Materials (CRM) since 2014; elemental phosphorus was added to the list in 2017 because its availability might be critically affected by the unstable geopolitical situation that characterizes the major global phosphorus suppliers.[1]

At present, phosphate rock reserves are largely concentrated in Morocco (about 77%), followed by China with less than 6% of the global total Fig. 2.[2]

The quantification of phosphorus and its compounds is crucial in many sectors: from the quality control of fertilizers and industrial products to the environmental assessment of soils and waters, up to applications in the biomedical and livestock fields. It is therefore necessary to have fast, reliable, and cost-effective analytical methods capable of providing timely information even directly in the field. At the same time, such methods should have a low environmental impact, reducing the use of chemical reagents, waste generation, and sample preparation times, in line with the principles of green chemistry.

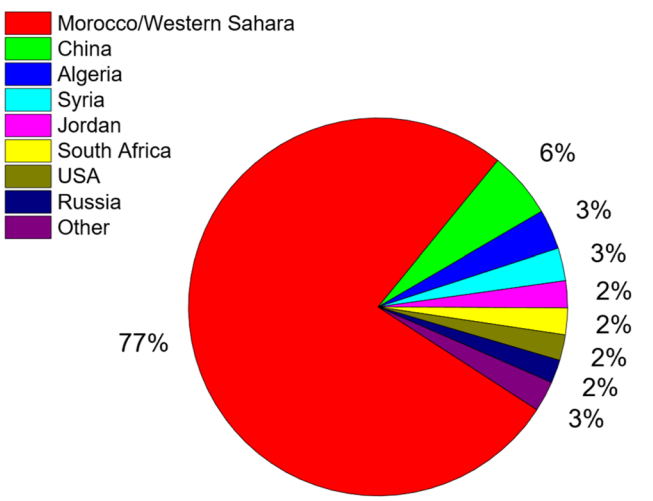

Fig. 2 Global distribution of phosphate rock reserves. Data derived from the U.S. Geological Survey (USGS) Mineral Commodity Summaries 2025.[2]

Traditional chemical techniques for phosphorus determination, such as colorimetric methods or acid digestion-based analysis followed by spectroscopy, often offer good accuracy and sensitivity but require laborious procedures, time-consuming processes, specialized personnel, and the use of potentially hazardous reagents. Moreover, such approaches are difficult to apply *in situ* and are poorly suited to contexts where frequent and large-scale monitoring is required.[8]

In this context, Laser-Induced Breakdown Spectroscopy (LIBS)[9] is emerging as an extremely promising analytical technique for the analysis of phosphorus and its compounds. LIBS is based on the generation of a micro-plasma by means of a laser pulse focused on the surface of the sample. The analysis of the light emitted by the plasma makes it possible to identify and quantify the elements present. Among the main advantages of LIBS are the speed of analysis, which can take place in seconds; the ability to perform near-non-destructive measurements; no or minimal sample preparation; and the ability to analyze solids, liquids, and gases. In addition, the technique does not require the use of chemical reagents, helping to reduce operating costs and environmental impact.

A further strength of LIBS is its suitability for the development of portable instrumentation for field analysis.[10] Compared to well-established portable techniques such as X-ray fluorescence (XRF), LIBS has specific advantages for phosphorus analysis. Firstly, it does not use ionizing radiation, eliminating the safety issues associated with the use of X-rays. Second, LIBS is more sensitive to light elements, such as phosphorus, which are often difficult to detect by XRF due to the low energy of the characteristic lines and the strong attenuation in materials and air. This makes LIBS particularly suitable for applications on soils, fertilizers, and biological materials, where phosphorus is present at varying concentrations.

The interest in the use of LIBS for the analysis of phosphorus and its compounds is demonstrated by the fact that the two papers in which the LIBS acronym was first introduced, published in 1981 by Loree and Radziemski,[11,12] mentioned as an example of a useful application of the technique the detection of phosphorus in DIMP (diisopropylmethyl phosphonate, $(C_3H_7)CH_3PO_3$), a surrogate for the chemical warfare gas sarin, as a marker for the identification of this molecule in gases.

Over the following decades, the interest in LIBS for phosphorus analysis progressively expanded from proof-of-concept studies to a broad range of applications involving environmental, agricultural, geological, industrial and biological matrices. This rapid evolution has been accompanied by the development of increasingly sophisticated experimental approaches and data-analysis strategies aimed at overcoming the analytical challenges associated with phosphorus determination.

In this review, we will discuss the most relevant contributions to the LIBS scientific literature on the applications of the technique to the analysis of phosphorus, with specific attention to the experimental approaches and the analytical methods developed in the last decade for overcoming or, at least,

reducing the negative effects of matrix variations on phosphorus quantitative analysis.

2. Materials and methods

The information about the literature on LIBS applications to phosphorus analysis has been retrieved from Scopus® searching for ("laser-induced breakdown spectroscopy" or "laser-induced plasma spectroscopy") and phosph* in the article title, abstract, and keywords. The search was limited to papers published before 31st December, 2025.

The search returned results related to applications of laser-induced breakdown spectroscopy (or laser-induced plasma spectroscopy, as the technique was often referred to in earlier literature) to phosphorus, phosphates, phosphate rocks, and related materials. The search reported 255 results, divided into 209 articles, 28 conference papers, 14 reviews, 3 book chapters, and 1 data paper.

The temporal evolution of the total number of publications, shown in Fig. 3, evidences a remarkable gap from the first 1981 Loree and Radziemski papers[11,12] and the one published in 1998 by the Laserna group in Malaga, Spain,[13] which is also the first paper published outside the USA on LIBS analysis of phosphorus.

The growth evidenced in the graph after 2000 reflects the expansion that the LIBS literature experienced after the first international LIBS Conference, held in Pisa, Italy, in October 2000.[14] The number of papers published in the literature demonstrates the consistent interest of the LIBS community in phosphorus analysis, particularly in fertilizers, soil, and plants, which align with the primary applications of this element.

A recent review[15] discussed advances in soil nutrient monitoring using various analytical techniques, including LIBS. The authors highlighted that one of the major challenges of using LIBS in complex matrices, such as soil, is the technique's high sensitivity to matrix variations, which can negatively affect its analytical capabilities.[16] The authors also noted significant improvements in LIBS analytical capabilities following the integration of chemometric, machine learning, and deep learning methods to support spectral analysis.

LIBS has greatly benefited from these techniques, perhaps more than other analytical methods, due to the intrinsic complexity of the relationship between measured line intensities and the concentration of the corresponding emitting elements. In LIBS, the relationship between intensity and concentration depends on factors such as the ablated mass, electron temperature, and electron number density.[17] These are global parameters of the plasma that depend not only on analyte concentration but also on the overall composition of the sample. For most LIBS applications in complex matrices, such as geological materials, biological samples, and soils, there is a consensus within the LIBS community that analytical approaches based on conventional calibration curves[18] should be replaced by multivariate methods.[19]

In the following sections, we therefore focus on recent advances in phosphorus analysis that exploit chemometric, machine learning, and deep learning approaches to overcome the limitations of conventional calibration strategies.

3. LIBS for phosphorus analysis

3.1 Analytical parameters for the detection of P

Phosphorus ($Z = 15$) belongs to the pnictogen group and has a single stable isotope, ^{31}P. Its electronic configuration ($1s^2 2s^2 2p^6 3s^2 3p^3$) and its relatively high first ionization energy

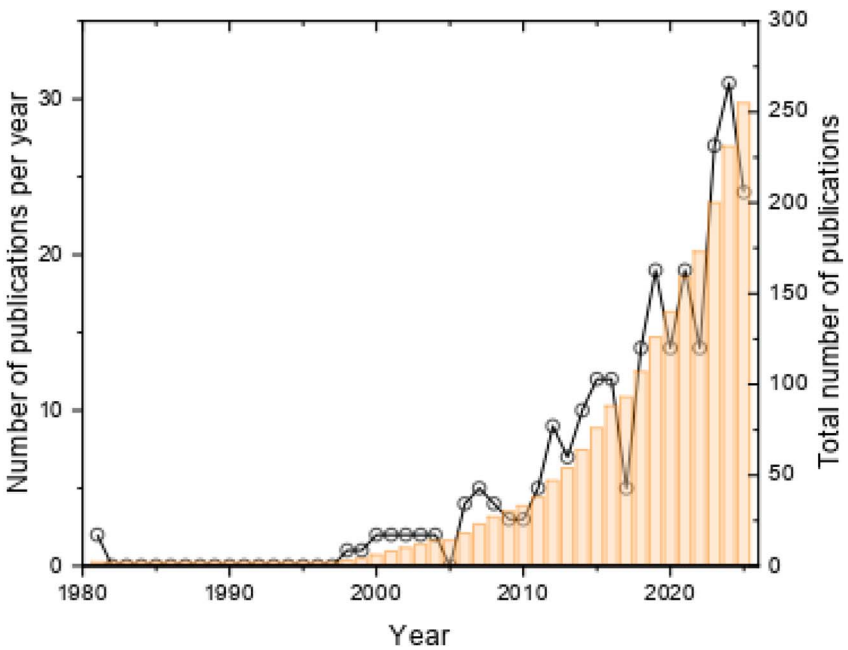

Fig. 3 Number per year (line and points, left scale) and total number (bars, right scale) of LIBS publications on phosphorus, from 1981 to 2025.

(10.5 eV) strongly influence its spectroscopic behavior in LIBS plasmas.

The main phosphorus lines in the LIBS spectrum are in the UV, corresponding to the emission of neutral phosphorus, whereas ionized phosphorus lines are visible between 440 and 560 nm, but they are considerably weaker than the neutral ones (Fig. 4).

It should be noted that the simulated spectra shown in Fig. 4 represent only the intrinsic atomic emission of phosphorus and do not account for the wavelength-dependent spectral response of the experimental detection system. In LIBS instruments, the overall detection efficiency, determined by the wavelength-dependent transmission of the optical components and the quantum efficiency of the detector, generally decreases significantly in the deep-UV region. Consequently, although the strongest P I spectral feature corresponds to the transition at 213.62 nm, this line may be less advantageous in practical applications than transitions at longer wavelengths, which benefit from higher overall detection efficiency and improved signal-to-noise ratios. The most intense P emission lines are reported in Table 1, together with their spectroscopic parameters.

Among the factors of merit used for measuring the quality of the results of an analytical technique, particularly important is the limit of detection (LOD), which corresponds to the minimum concentration of the analyte that can be detected using the technique with a reasonable probability. The formula usually applied for the LOD is given by the relation:

$$\mathrm{LOD} = \frac{3\sigma}{b} \tag{1}$$

where σ is the standard deviation of the signal measured on a blank (*i.e.*, at zero analyte concentration) and b is the slope of the calibration curve. It should be emphasized that eqn (1),

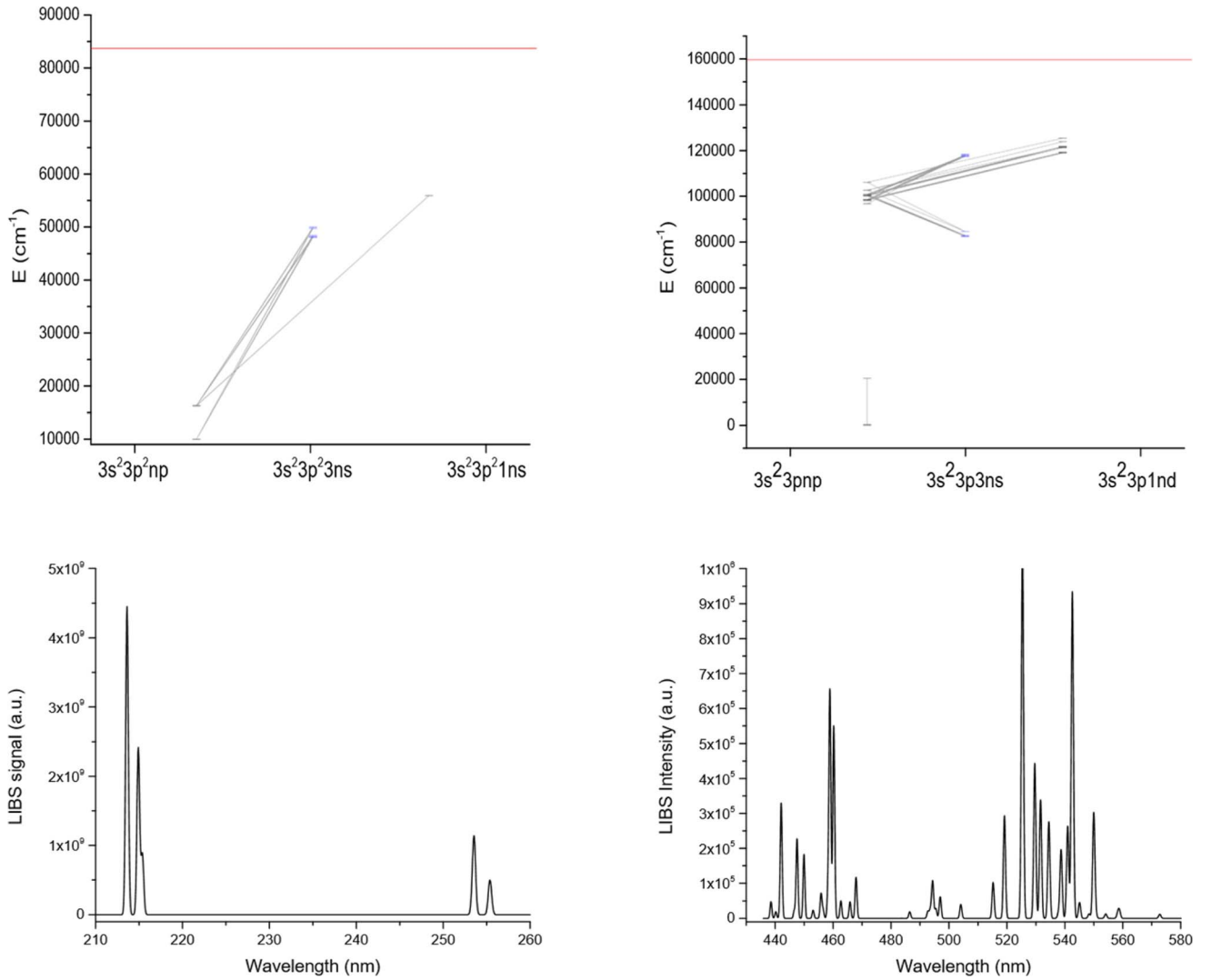

Fig. 4 Top: Grotrian diagram for neutral phosphorus (PI) (left) and for ionized phosphorus (PII) (right); in red, the ionization energies. Bottom: Simulated spectra for neutral phosphorus (left) and for ionized phosphorus (right). The figures were generated using data from the NIST Atomic Spectra Database[20] and the NIST LIBS Database.[21] Simulated spectra correspond to electron temperature $T = 1$ eV and electron number density $n_e = 1 \times 10^{17}$ e cm^{-3}.

Table 1 The most intense phosphorus emission lines and their spectroscopic parameters.[20]

	Wavelength (nm)	E_i (eV)	E_k (eV)	g_i	g_k	A_{ki} (s^{-1})
P I	213.55	1.41	7.21	4	4	2.11×10^7
	213.62	1.41	7.21	6	4	2.83×10^8
	214.91	1.41	7.18	4	2	3.18×10^8
	215.29	2.32	8.08	2	4	4.85×10^7
	215.41	2.32	8.08	4	6	5.8×10^7
	223.57	1.41	6.95	6	4	6.2×10^5
	253.40	2.32	7.17	2	4	2.0×10^7
	253.56	2.32	7.21	4	4	9.5×10^7
	255.32	2.32	7.17	2	2	7.1×10^7
	255.49	2.32	7.17	2	2	3.0×10^7

which follows the operational definition of the LOD recommended by the International Union of Pure and Applied Chemistry (IUPAC),[22] generally provides an optimistic estimate of the actual detection capability under typical LIBS operating conditions. As discussed in our previous work,[23] a rigorous formulation of the problem can provide a more realistic estimate of the achievable detection limit. Nevertheless, eqn (1) has been retained in this review because it is by far the most widely adopted expression in the LIBS literature, including the great majority of publications dealing with phosphorus determination, thus allowing a consistent comparison among the reported analytical performances.

An important analytical indicator is the root mean square error (of prediction) (RMSE), which is associated with the analytical precision of the technique, and is defined as:

$$\mathrm{RMSE} = \sqrt{\frac{\sum_{i=1}^{n} (p_i - r_i)^2}{n}} \tag{2}$$

where n is the number of samples, p_i are the predictions obtained from the experiment and r_i are the corresponding reference values.

Other figures of merit include the slope b of the predicted-*versus*-reference calibration and the correlation coefficient R^2, defined as:

$$R^2 = 1 - \frac{\sum_{i=1}^{n} (p_i - r_i)^2}{\sum_{i=1}^{n} (p_i - \bar{p})^2} \tag{3}$$

where n is the number of samples, p_i are the predictions obtained from the experiment, r_i are the corresponding reference values and $\bar{p}$ is the mean of the experimental predictions.

The slope (b) of the predicted-*versus*-reference calibration curve provides an estimate of the accuracy of the quantitative method. Ideally, $b = 1$ indicates perfect agreement between predicted and reference concentrations, whereas deviations from unity may reveal a systematic bias in the predicted values.

Other parameters that are often used[24] are the mean absolute error (MAE):

$$\mathrm{MAE} = \frac{\sum_{i=1}^{n} |(p_i - r_i)|}{n} \tag{4}$$

The mean absolute percentage error (MAPE):

$$\mathrm{MAPE} = \frac{100}{n} \sum_{i=1}^{n} \left| \frac{(p_i - r_i)}{p_i} \right| \tag{5}$$

And the mean squared error (MSE):

$$\mathrm{MSE} = \mathrm{RMSE}^2 \tag{6}$$

Due to its intrinsic versatility, LIBS has been applied to phosphorus analysis in many different contexts; most of the papers dealt with the use of phosphorus in agriculture, measuring its concentration in fertilizers, soils, and plants. Other studies also focused on the use of organic materials as alternatives to phosphate rock or analyzed phosphorus from a geological perspective. In the following sections the most recent advances in these fields are presented, evidencing the experimental and analytical strategies used and the main results obtained.

3.2 Agricultural matrices: opportunities and matrix-related limitations

Agricultural matrices represent one of the most important application areas for LIBS phosphorus analysis, but they also highlight many of the intrinsic limitations of the technique, particularly those related to matrix variability and calibration transferability.

The use of LIBS for the analysis of agricultural materials and food has been the subject of an extensive review, in two parts, by Nicolodelli *et al.*[25] and Senesi *et al.*,[26] in which the authors discussed several papers dealing with phosphorus analysis in the 2010–2019 decade.

3.2.1. Fertilizers: one of the most favorable matrices for LIBS quantification. Compared with soils or biological samples, fertilizers often represent a relatively favorable class of matrices for LIBS quantification, although matrix-related effects still play a significant role in analytical robustness. One of the first applications of chemometric techniques to the LIBS analysis of phosphorus is reported in a study on fertilizers published in 2010 by Li *et al.*[27] The authors used a multivariate linear method called Partial Least Square (PLS) analysis to build a robust calibration model for the determination of phosphorus and potassium in fertilizers, after verifying that a conventional univariate calibration curve approach based on the intensity of the P I line at 213.55 nm was not yielding acceptable results. In PLS, a multivariate (linear) calibration model is built by considering a linear combination of several spectral features, including spectral lines not belonging to the analyte under study, to consider, although only linearly, the effect that changes in the sample matrix would have on the analytical line emission. In particular, the authors verified that Mg, Ca, and N lines (and thus, concentration) affected both P and K emission

lines, while the correlation between phosphorus and potassium emission was negligible. The authors finally estimated an absolute error on P concentration (converted to P_2O_5 oxide) of the order of 0.3 wt% for P_2O_5 concentrations around 10 wt%, with a relative standard deviation (RSD), calculated on 3 independent measures of less than 5%.

Marangoni *et al.*[28] used a different strategy for overcoming matrix effects in the analysis of fertilizers. They normalized the intensity of the phosphorus line at 213.62 nm with the continuous background signal under the curve to reduce the effect of the ablated mass variations (physical matrix effect). The chemical matrix effects[16,29] due to changes in electron temperature and number density were not corrected; however, the reported overall precision of the method, with a relative RMSE < 15% and a LOD of 0.5 wt% P, was considered satisfactory.

Nicolodelli *et al.*[30] explored the possibility of using double-pulse LIBS (DP-LIBS) analysis for determining macro- and micro-nutrients in organic fertilizers. DP-LIBS is a variation of the conventional LIBS technique in which the laser pulse is divided into two suitably retarded pulses. Different DP geometries have been studied in LIBS literature (collinear or parallel pulses, pre-ablation or reheating orthogonal pulses).[31] The authors used a collinear configuration, which is the most effective in terms of signal enhancement, and is due to the creation of a reduced density environment inside the shock wave produced by the first pulse, so increasing the ablation rate of the second laser pulse.[32] The authors observed a large enhancement of most of the LIBS emission lines, whereas the best LOD obtained for phosphorus was achieved by building a conventional univariate calibration curve using the P I line at 213.81 nm (about 900 ppm *versus* about 2400 ppm determined in single pulse mode).

Senesi *et al.*[33] used multivariate methods such as principal component analysis and PLS regression to discriminate fertilizers of different nature, obtaining their classification at a 95% confidence level.

In 2019, Zhang *et al.*[34] compared the analytical capabilities of the univariate calibration curve using the 213.62 nm P I emission line with 212.41 nm Si I normalization *versus* a multivariate approach (PLS) for measuring phosphorus concentration in fertilizers. They found that PLS provided better analytical results than the univariate approach, with RMSE < 0.15% and RSD slightly higher than 5%.

In the same year, Sha *et al.*[35] used a support vector machine (SVM) regression model for quantitative analysis of nutrients in 58 fertilizer samples. SVM[36] is a nonlinear machine learning technique that operates a projection of the input data (the LIBS spectral features) in high-dimensional feature space, where a hyperplane with minimum predictive error is found. When compared with conventional univariate calibration curve analysis based on the intensity of the P I line at 213.62 nm, the authors evidenced that SVM regression had a better determination coefficient ($R^2 = 0.993$ with respect to $R^2 = 0.909$ of the univariate calibration curve) with an RMSE of the predicted concentration equal to 0.026 wt%.

Vieira *et al.*[37] and Dib *et al.*[38] analyzed the phosphorus content in conventional and biochar-based fertilizers using a combination of LIBS and spark discharge, suitably delayed with respect to the laser pulse to reheat the plasma and, consequently, to enhance the LIBS signal. The authors used a conventional univariate approach, using either the intensity of the P I 214.91 nm emission line,[37] or the total intensity of the P I unresolved lines at 253.40 and 253.55 nm[38] in a linear range of phosphorus concentration from 0.71 wt% to 11.73 wt% with $R^2 = 0.9957$ and a LOD of 0.21 wt%. The results obtained on three biochar-based fertilizers using this calibration curve showed no statistical difference from the reference values determined by conventional chemical methods, at a 99% confidence level.

Babos *et al.*[39] proposed the use of LIBS and digital image data fusion for the determination of Al, Ca, Fe, Mg, and P contents in mineral fertilizer. These authors observed a marked reduction, around 20%, of the prediction errors when using data fusion with respect to multivariate linear analysis using LIBS data only.

More recently, Zhong *et al.*[40] used a handheld LIBS instrumentation for the characterization of fertilizers based on the main nutrient content. The authors used a Euclidean distance prediction algorithm with PLS regression, obtaining for the analysis of phosphorus a determination coefficient $R^2 = 0.9541$ with RMSE = 1.02 g kg^{-1} and an RSD = 4.64%.

Overall, the studies discussed in this section demonstrate that LIBS is capable of providing reliable phosphorus quantification in relatively homogeneous solid matrices when appropriate calibration strategies are adopted. However, matrix-dependent effects remain the principal source of uncertainty, limiting the transferability of calibration models and emphasizing the need for robust correction procedures.

3.2.2. Soils and water: quantitative phosphorus analysis in complex matrices. Soils probably represent the most challenging matrices for phosphorus quantification by LIBS because of their strong physical and chemical heterogeneity. For this reason, this field has become one of the main testing grounds for multivariate and machine-learning approaches.

In 2013, Lu *et al.*[41] used LIBS in conjunction with suitable calibration models to ascertain the total phosphorus (TP) content in seven soil samples and the total nitrogen (TN) content in ten soil samples. The TN and TP contents ascertained by conventional chemical analysis techniques had a high linear correlation with the LIBS data. As a result, when calibration and validation samples with comparable matrix compositions were examined, LIBS proved to be an effective method for identifying N and P in soils.

In 2019, Xu *et al.*[42] used PLS regression for evaluating many important parameters in soil analysis, including TP and available phosphorus (AP), from the LIBS spectra. As expected, the evaluation of AP was poor, since LIBS is an elemental technique not suitable for the speciation. On the contrary, TP was evaluated satisfactorily, together with other parameters such as soil organic matter (SOM), TN, and total potassium (TK). The authors noted that a PLS approach using only the spectral data belonging to P lines was less accurate than the model built using the full spectrum. They also noted a correlation between P concentration and the intensity of the emission lines of elements such as K, Ca, Al, Fe, C, N, and O, with which

phosphorus is linked in soil (inorganic phosphorus linked to K, Ca, Al, Fe and organic phosphorus to C, N and O).

In 2022, Xu *et al.*[43] used a deep learning end-to-end soil analysis based on Convolutional Neural Networks (CNN) which are an evolution of conventional Artificial Neural Networks (ANN), sharing with them the possibility of modelling non-linear multivariate relations between LIBS spectral features and elemental concentrations, but characterized by a better generalization capability. The authors determined from the LIBS spectrum the values of pH, SOM, TN, TP, and TK in the soil. In comparison with PLS analysis, the RMSE of these parameters was consistently lower, with the TP RMSE being the highest (10%) among all the parameters considered. Moreover, the authors noted that there was no visible phosphorus line in the LIBS spectra; however, other elements' spectral lines showed a correlation with phosphorus concentration, this because the same correlation might exist between the elements' concentrations in the samples used for training. This indirect relationship between different elements concentrations is often interpreted as a strong point in favor of the use of multi-elemental algorithms in the analysis of complex matrices. On the contrary, the apparent 'determination' of an element concentration solely from the emission lines of other elements may largely reflect correlations embedded in the training dataset rather than true spectroscopic sensitivity to the analyte. If the reference samples are not fully representative of the unknowns, the results obtained can be completely wrong. In other words, matrix changes between reference and unknown samples would not be compensated even if the multielemental algorithm had potentially the capability to do so.

Soni *et al.*[44,45] measured the TP concentration in 12 soil samples of different matrix composition using LIBS and Laser-Induced Fluorescence (LIF). The authors used a conventional LIBS setup for creating the plasma, together with a tunable laser to selectively stimulate the 253.56 nm P I transition. The resulting fluorescence signal at the 213.62 nm wavelength was strongly enhanced and free from spectral interferences. Although this method did not directly compensate for matrix effects, the resulting calibration curves for clay soils (>30% clay particles) and silt loam/loam soils (<30% clay) were characterized by better determination coefficients and much lower LODs (<0.3 mg kg^{-1}, about 40 times lower with respect to LIBS alone).

Sánchez-Esteva *et al.* (2020)[46] used LIBS, visible near-infrared spectroscopy (vis-NIRS), and their combination to quantify various soil P pools, including TP, water-extractable P, Olsen P, and oxalate-extractable P (Pox). Partial least squares regression (PLSR) modeling was used by testing and comparing the two variable selection techniques, interval partial least squares (iPLS) and competitive adaptive reweighted sampling (CARS). LIBS was shown to outperform vis-NIRS in nearly every model and soil P pool. Furthermore, the variable selection improved significantly the model for both spectroscopic methods and their combination. Besides picking, on average, five times fewer variables and exhibiting quicker computing time, the CARS variable selection method greatly outperformed iPLS, leading to a generally improved model performance. In comparison to iPLS, the modeling process and model complexity were significantly decreased by the CARS variable selection method. The characteristic P I emission lines at 213.62, 214.91, and 215.41 nm, as well as the regions between 400 and 600 nm, which are linked to Fe-oxides and various functional groups of SOM, and between 2300 and 2400 nm, which are linked to O–H bonds, seemed to be the most pertinent spectral regions for P modeling. With the exception of oxalate-extractable P, which yielded results comparable to LIBS models with CARS, the combined LIBS and vis-NIRS models with variable selection yielded the best results for all four P pools. In comparison to all the other P pools, Pox was also found to achieve the lowest standard RMSE. Overall, the combination of LIBS and vis-NIRS with variable selection proved to be very promising for improving soil P measurements.

Al-Juboori *et al.*[47] investigated the influence of organic and inorganic fertilizers, including phosphorus, triple superphosphate, compost, or compost + triple superphosphate, on the availability and distribution of phosphorus in soil. The authors tried to determine the phosphorus concentration in the samples using the intensity of the P I line at 253.56 nm. However, the results obtained were not conclusive, with the highest phosphorus line intensity observed in the untreated soil. However, the authors also noticed that the intensity ratio between the two neutral phosphorus lines at 253.56 nm and 255.32 nm was varying from sample to sample. Since these lines have different upper energies (see Table 1), the variation of the intensity ratio is the result of changes in the plasma electron temperature due to the different matrices of the samples and/or laser intensity fluctuations. In this case, a calibration-free approach on spectra acquired in a proper narrow time window would probably improve the interpretability of results.

Erler *et al.* (2020)[48] determined the major (N, Mg, P, K, and Ca) and minor (Mn and Fe) nutrient element concentrations, TP and TA abundances, humus content, and pH of 137 topsoil samples taken from two agricultural fields in Germany using a commercial handheld LIBS device. Three different multivariate regression methods, *i.e.*, PLSR, least absolute shrinkage (Lasso) and Gaussian process regression (GPR) were characterized and compared for measuring soil parameters. Furthermore, several methods of data pretreatment, namely variance reduction, background correction and normalization, were tested. The latter method in particular showed the potential of yielding improved multivariate regression results. The qualitative correlation between predicted and observed P values achieved with Lasso was $R^2 = 0.21$, and similar values, *i.e.*, $R^2 = 0.14$ and $R^2 = 0.28$, were achieved with PLSR and GPR.

In a recent paper, Zhang *et al.*[49] analyzed the presence of phosphorus in water using a strategy based on the conversion of the liquid sample into a solid one. Direct analysis of liquids by LIBS is problematic because of the occurrence of surface ripples and splashing in the interaction of the laser beam with the liquid surface. Through liquid-to-solid conversion, the analysis is reduced to a conventional LIBS measurement on a solid sample. A conventional calibration approach, using the P I lines at 213.62 nm and 214.91 nm and the carbon line at 247.86 nm for normalization, allowed the authors to obtain R^2 values of 0.981 and 0.993 and LOD values of 0.09 mg L^{-1} and 0.23 mg L^{-1},

respectively. Furthermore, the authors compared the calibration curve results with the prediction of a combined PLS-SVM model. Using the multivariate approach, the average error on phosphorus concentration prediction was reduced from about 12% to less than 4% on the test samples.

Another promising approach for the analysis of phosphorus in water has been proposed by Yang and co-workers, who introduced a plasma amplification LIBS (PA-LIBS) method.[50] They achieved a substantial improvement in analytical sensitivity through plasma enhancement. The same research group subsequently refined the technique by optimizing the aerosol temperature.[51] With increasing the liquid aerosol temperature, the emission intensity of P increased and the LOD of P decreased from 5.22 to 1.81 ppm. Furthermore, the R^2, the average relative error (ARE), and the root mean square error of cross validation (RMSECV) were improved from 0.9926 to 0.9964, 8.93 to 5.95%, and 4.85 to 2.91 ppm, respectively. More recently, by introducing spatially resolved detection and improved plasma-generation conditions, the authors further extended the analytical performance of the method.[52,53] These developments demonstrate the rapid evolution of source-assisted plasma enhancement strategies for LIBS analysis of aqueous samples.

These investigations confirm that increasing matrix complexity generally leads to a progressive deterioration of analytical performance. Consequently, calibration approaches specifically designed to compensate for matrix-dependent effects become essential for obtaining reliable quantitative results.

3.2.3. Biological matrices and indirect correlations in multivariate models. Biological matrices further complicate LIBS phosphorus analysis because spectral variations may reflect both elemental composition and complex biochemical correlations within the samples.

In 2014, Ma and Dong[54] used chemometric methods (PCA) for detecting traces of the chlorpyrifos pesticide residues on apples. They used the intensity of the phosphorus (213.62 and 214.91 nm), sulfur (393.33 and 396.89 nm), and chlorine (837.59 nm) emission lines for discriminating between treated and untreated apples. The authors found that the phosphorus lines could be detected even after spraying the apples with a pesticide diluted down to a 1 : 100 ratio, although they were not able to obtain any reliable quantitative results.

Devey *et al.*[55] in 2015 analyzed pasture-based plants for several nutrient elements, including phosphorus, obtaining LODs of the order of a few mg kg^{-1}, with relative errors for phosphorus < 0.02%.

In the same year, Arantes de Carvalho *et al.*[56] determined the nutrient profile of 31 plant samples, covering a wide range of matrices using nanosecond (ns) and femtosecond (fs) LIBS. The LOD for P resulted lower when using ns-LIBS, *i.e.*, 0.1 g kg^{-1} *versus* 0.7 g kg^{-1} achieved by fs-LIBS, due to the more intense signals obtained. However, for ns-LIBS a conventional univariate calibration curve analysis, which used the 213.62 nm line for phosphorus quantification, was not yielding acceptable results. However, when treated with chemometric methods (PLS analysis) ns-LIBS spectra provided results comparable to fs-LIBS only. The authors concluded that fs-LIBS provides marginally better results because the decoupling between laser irradiation and plasma formation results in a reduced sensitivity to matrix effects. On the other hand, the use of multivariate analysis allowed to achieve results similar to those achieved by ns-LIBS. This result, together with the better LOD observed, would suggest that ns-LIBS is preferable to fs-LIBS for the determination of nutrient profile in plants.

In 2019, with the intent to overcome the matrix effect, Babos *et al.*[57] proposed two different strategies for the analysis of phosphorus in solid mineral supplements for cattle, based on multi energy calibration (MEC) technique[58] and one-point gravimetric standard addition (OP GSA).[59] In theory, the MEC method requires only a single reference material with a known composition together with a "blank" sample, that is, a material containing no analyte, to quantify phosphorus in samples of unknown concentration. The procedure consists of preparing two blends: the first obtained by combining the standard and the blank in equal mass proportions (50/50), while the second produced by mixing the same standard with the unknown sample in the same ratio. Depending on the application, other mixing proportions may also be adopted. Both mixtures are then analyzed under identical experimental conditions, and the LIBS emission intensities of two or more phosphorus spectral lines are measured. For each selected line, the intensity measured for the "standard + blank" mixture is plotted along the horizontal axis (as a function of line energy), whereas the corresponding intensity from the "standard + unknown" mixture is plotted on the vertical axis. If the LIBS response varies linearly with analyte concentration, the resulting points should align on a straight line whose slope, S, can be used to calculate the phosphorus content of the unknown sample (C_{unk}) from the content of the standard (C_{S}) according to eqn (7).

$$C_{\mathrm{unk}} = \frac{S}{1 - S} C_{\mathrm{S}} \tag{7}$$

From eqn (7) it appears that this strategy is essentially a lengthier and more elaborate version of the conventional single-standard calibration approach. Consequently, possible matrix effects are not compensated, since the derivation of eqn (7) assumes that the proportionality between the LIBS signal and analyte concentration is identical for both the standard and the unknown matrix.

Similar drawback characterizes the second approach proposed by the authors and referred to as one-point gravimetric standard addition. In this case as well, two mixtures are prepared by combining the standard in equal mass fraction (50%) with either the blank or the unknown sample. The analysis is restricted to a single emission line of the analyte. Denoting by $I_{(\mathrm{S+B})}$ the measured intensity for the standard–blank mixture and by $I_{(\mathrm{S+unk})}$ the intensity for the standard–unknown mixture, the analyte concentration in the unknown is calculated using:

$$C_{\mathrm{unk}} = \left(\frac{I_{\mathrm{S+unk}}}{I_{\mathrm{S+B}}} - 1 \right) C_{\mathrm{S}} \tag{8}$$

Like the MEC approach, eqn (8) is derived under the assumption of a linear dependence of the LIBS signal on analyte concentration. As a result, this method cannot be regarded as an effective strategy for compensation of matrix effects.

It is worth emphasizing that the above conclusion should not be interpreted as a limitation of the standard addition method itself, which has long been recognized as one of the most powerful and reliable approaches for compensating matrix effects in analytical chemistry. The limitation concerns only the simplified MEC and one-point gravimetric procedures discussed above, whose derivation still assumes an identical proportionality between analyte concentration and LIBS signal in both the reference and unknown samples. In contrast, the classical standard addition method does not rely on this assumption and has proven highly effective in minimizing matrix-dependent biases. Although its application to phosphorus determination by LIBS is still relatively limited, a comprehensive review by Yang and co-workers[60] has highlighted the growing interest in adapting standard addition strategies to LIBS for improving quantitative accuracy in complex matrices.

In the same year, in an effort to improve LIBS performance, Zhao *et al.* (2019)[61] employed the recently developed nanoparticle-enhanced (NE) LIBS system to measure chlorpyrifos residues on apple and chive fruit surfaces, and Cd in lettuce. Samples were chopped into pieces, dropped with chlorpyrifos solution at different concentrations, covered with an 80 nm Ag nanoparticle solution, and then dried in order to get the NE LIBS and standard LIBS spectra. Compared to chive samples, the P signals of apple samples achieved by NE LIBS were more enhanced and more intense than those obtained by normal LIBS. On the other hand, the P signals on the surfaces of chives were about twice as strong as those on the surfaces of apples, suggesting that chlorpyrifos was easier to detect on chives than on apples. The plot of the intensity of the distinctive P peaks at 213.62, 214.91, 253.56, and 255.33 nm *versus* the concentration of chlorpyrifos yielded calibration curves that showed a strong positive correlation, with the most stable P line at 214.91 nm producing the strongest correlation. Using the four P lines, NE LIBS achieved chlorpyrifos LODs of 0.019, 0.015, 0.009, and 0.029 wt%, which were two orders of magnitude lower than those achieved by normal LIBS.

Gamela *et al.*[62] combined LIBS and Wavelength-Dispersive X-ray fluorescence (WD-XRF) to determine the concentration of potassium, magnesium, and phosphorus in bean seeds. The authors demonstrated that a multivariate approach that uses the combined information of the two techniques yielded better results than single LIBS or XRF analysis. The authors reported an average error of 0.10% and a recovery ranging between 73 and 128% for phosphorus in bean seeds of different species, where P concentration ranged from 0.27% to 0.82%.

Aldakheel *et al.*[63] used LIBS together with X-ray photoelectron spectroscopy (XPS) and inductively coupled plasma-optical emission spectroscopy (ICP-OES) for the analysis of major and minor components of *Moringa oleifera* (drumstick tree) leaves. The leaves of *Moringa oleifera* are used in traditional Asian medicine for diabetes treatment and are also reputed to be effective for antimicrobial and pharmacological applications as supplements and growth promoters. The authors used Calibration-Free LIBS (CF-LIBS) for determining the leaves' elemental composition, and compared the results obtained with that of XPS and ICP-OES analysis. The electron temperature was evaluated from the Boltzmann plot[64] of Ca I emission and also used the Ca I emission line at 442.50 nm was used for determining the electron number density from the measurement of the Stark broadening[65] of the line. Despite the apparently good agreement of the P concentration calculated by CF-LIBS and the one determined by ICP-OES (2.7 g L^{-1} and 2.8 g L^{-1}, respectively), it should be remarked that the application of CF-LIBS to time-integrated spectra, as done by the authors, is not possible,[66] since CF-LIBS is based on the hypothesis of having the plasma in Local Thermal Equilibrium (LTE) conditions[67] and these conditions are typically valid only in a narrow time interval during plasma evolution. Moreover, the plasma electron temperature and number density must be defined in a time interval short enough to guarantee that these quantities would not change appreciably during the measurement.

Erler *et al.* (2020)[48] used a commercially available handheld LIBS instrument coupled with three different multivariate regression methods (PLSR, Lasso and GPR) to investigate the plant available mass fraction of P. The best correlation was obtained by GPR with $R^2 = 0.35$, which is a first proof-of-principle for predicting plant available nutrient contents based on LIBS. Slightly worse predictions were achieved by using Lasso, $R^2 = 0.25$, and PLSR, $R^2 = 0.22$. Noteworthy, the prediction of P available for plants was better than the prediction of the total P content.

The use of phosphates in seafood as an additive is legitimate for preserving its moisture and maintaining its organoleptic properties However, an excessive use of these additives, aimed at fraudulently increasing the weight and size of the product, has raised some concern. In 2021, Tian *et al.*[68] used LIBS and machine learning for the quantitative determination of phosphorus in seafood. By comparing the results of PLS and SVM methods with a univariate calibration curve built using the P I line at 253.56 nm (with or without normalization by the C I 247.86 nm line), the authors found that the latter approach was very sensitive to matrix variation (different calibration curves were built according to the types of seafood analyzed). Differently, PLS and SVM were able to build matrix-independent models, with SVM outperforming PLS in terms of RMSE (1.42 g kg^{-1} *versus* 1.68 g kg^{-1}) and average RSD (5.2% *versus* 9.4% of PLS).

Martin *et al.*[69] analyzed switchgrass biomass by LIBS for determining the quality of the feedstock in terms of its inorganic composition. The concentration of major micronutrients such as silicon, potassium, calcium, magnesium, phosphorus, and sulfur were determined by PLS analysis. In the case of phosphorus, a RMSE slightly higher than 80 ppm was achieved for P concentrations ranging from 200 to 1400 ppm. However, these results must be interpreted with care, as the PLS method calculates the concentration of the elements based on spectral features, which in principle cannot be related to the analyte emission. The relation between these features and the analyte

concentration is indeed determined through a calibration process using reference samples of known composition. If for the calibration samples a correlation exists between the concentrations of two elements, one of them can be 'determined' from the spectral features of the other, even if its emission lines are not visible in the LIBS spectrum. In this work, this problem is evidenced for sulfur, which is 'determined' in the samples at concentrations and with RMSE similar to those of phosphorus. The emission lines of sulfur are not visible in the spectrum, but the sulfur concentration in the calibration samples is strongly correlated with that of potassium, magnesium, and phosphorus. The results reported should be thus taken with care, especially if the representativity of the reference samples is not well ascertained.

Sezer *et al.*[70] applied LIBS for discriminating Kashar cheese (a pasta-filata cheese typical of Turkey) from industrially processed cheese, based on the spectral information from Mg, Ca, Na, P, Zn, and K emission lines in the spectrum. The spectral lines of these elements were found to be substantially higher in industrial processed cheese with respect to Kashar cheese, which suggested a higher concentration of these elements in industrial processed cheese. The quantitative analysis of cheese composition was done using PLS regression, and phosphorus results were the most precise ones among the elements considered, with $R^2 = 0.965$, RSD = 1.03%, REP = 1.07%, RMSE = 51.45 and LOD = 33.4 ppm.

Nouman Khan *et al.*[71] used chemometric techniques for the evaluation of major and minor nutrients in the root, leaves, and seeds of several medicinal plants (*Taraxacum officinale*, *Hyoscyamus niger*, *Ajuga bracteosa*, *Elaeagnus angustifolia*, *Berberis lyceum*, and *Camellia sinensis*). The elements Ca, Mg, Si, and P were the major ones detected in all the samples, so allowing to classify with an accuracy of 95% the medicinal plants according to their content using PLS analysis. The line used for phosphorus detection was the atomic phosphorus line at 533.24 nm.

Finally, Steen *et al.*[72] exploited the elemental imaging capabilities of LIBS[73–76] for mapping the distribution of several elements, including phosphorus, in cocoa beans. The intensity of the P I line at 213.62 nm (normalized to the C I line at 247.86 nm) was used as an indication of the phosphorus content at the point of analysis. The authors remarked that the density of the organic material would vary considerably within the seed, with an inner structure showing a very low melting point. When this matrix variation was mitigated using roasted seed, the LIBS analysis required about 90 minutes (about one second per point) for scanning a single seed (about 30 mm × 20 mm). The spacing between the laser shots was 300 microns, while the diameter of the LIBS crater was only 45 μm, thus leaving room for further improvements in elemental imaging resolution. The authors noted that the overall resolution of the elemental maps was in general lower than the one obtained using micro-XRF. However, LIBS micro-imaging is faster and sensitive to low-*Z* elements that are not detectable using XRF. Despite the low intensity of the phosphorus line, the phosphorus elemental map evidenced a higher accumulation of the element in the germ of the seed together with magnesium, while manganese, iron, and zinc signals are more pronounced in the shell.[72]

3.2.4. Secondary resources and highly heterogeneous matrices. Waste-derived materials represent particularly difficult matrices because of their high heterogeneity and variable mineralogical composition, making them ideal case studies for testing model robustness and transferability.

In 2022, Elsayed *et al.*[77] used a CF-LIBS approach for determining the concentration of phosphorus in phosphogypsum waste, ($CaSO_4$) which is a byproduct of the treatment of phosphate rocks with sulfuric acid for producing phosphoric acid. The composition of this material is very complex due to the presence of impurities and contaminants, thus only 15% of phosphogypsum produced in phosphate rock processing is recycled in agriculture or as a building material. Given the interest in the study of this material, the authors[77] used conventional univariate curves for determining the phosphorus concentration from the intensities of the P I lines at 213.61 nm, 214.91 nm and 215.40 nm. Moreover, they found a linear correlation between the global plasma parameters (electron temperature and number density), determined using the CF-LIBS algorithm, and the phosphorus concentration in the waste, which suggested an alternative approach for evaluating phosphorus concentration based on plasma parameters rather than directly on phosphorus line intensities. This approach, if confirmed by further experiments, could be interesting because the experimental determination of the electron number density from the Stark broadening of the emission lines does not depend on the hypothesis of plasma in LTE, thus opening the possibility of use of a CF-LIBS-like approach even in the absence of LTE conditions.

Massa and co-workers[78] introduced an alternative strategy for assessing phosphorus levels in sewage sludge ash (SSA) by combining portable LIBS measurements with deep learning techniques. SSA, which is generated during the thermal processing of wastewater residues, represents a valuable secondary phosphorus resource because its phosphorus content is comparable to that of low-grade phosphate ores. In this study,[78] LIBS spectra were collected using a handheld LIBS device, which enabled rapid data acquisition but limited the accuracy achievable through the instrument's built-in quantification routines. To overcome this limitation, the authors implemented a CNN trained on LIBS spectra from laboratory-prepared standards containing known phosphorus concentrations. To improve robustness, the training dataset was further expanded through spectral data augmentation.[79] Noteworthy, during model training, validation was carried out using spectra from a small number of real SSA samples that were characterized independently. These samples, which featured a much more complex and heterogeneous matrix than that of synthetic standards, provided a demanding benchmark for evaluating the model's applicability in practical scenarios.

In particular, the CNN architecture was tuned by minimizing the root mean square error between predicted and measured phosphorus contents in the SSA validation set. This optimization approach ensured that the model achieved not only a strong agreement with the reference standards, but also reliable performance on real samples. The resulting CNN clearly

outperformed both a simple univariate calibration and a conventional artificial neural network, the latter failing to build a model transferable between synthetic and real SSA data. In contrast, the CNN delivered accurate predictions for both datasets, indicating its ability to extract spectral features that remain robust despite significant matrix variations. A coefficient of determination of $R^2 = 0.96$, with RMSE = 0.9%, was achieved.

Overall, the studies reviewed in Section 3.2 demonstrate that LIBS has become a mature analytical technique for phosphorus determination in a wide variety of matrices. Although satisfactory quantitative performances have been reported in many applications, the analytical accuracy remains strongly dependent on matrix composition, sample heterogeneity, and calibration strategy. These common issues emerge consistently across the different application fields and motivate the development of more advanced approaches for matrix-effect compensation, signal enhancement, and data processing, which are discussed in the following sections.

3.3 Geological applications and field-portable LIBS

Geological applications have played an important role in the development of portable and stand-off LIBS instrumentation, where robustness and rapid classification are often more important than absolute quantitative accuracy.

One of the first works on the application of field portable LIBS system to the analysis of phosphate ores was developed by Rosenwasser *et al.* (2001),[80] who successfully used the equipment provided with an installed auto sampler on-site for ore grading at the Smokey Canyon phosphate mine in Idaho (USA) with a respectable degree of accuracy and precision. Methods were developed to automatically perform metallic element calibrations for supplied phosphate ore samples containing known concentrations of the following minerals: P_2O_5, CaO, MgO, SiO_2 and Al_2O_3. Calibrations were achieved for P, Ca, Mg, Al and Si with linear regression coefficients of 0.985, 0.980, 0.993, 0.987 and 0.985, respectively. The preparation and analytical time for each sample was less than 5 min.

Some years later, in 2006, Asimellis *et al.*[81] determined the ratio between the average of the 213.62 nm and 214.92 nm P I lines to the Si I line at 212.41 nm, using it as a proxy for the actual P/Si concentration ratio, which is considered a reliable indicator of ore rock quality. An acceptable correlation was found between measured and supplied analytical data, which allowed them to easily discriminate high-quality from low-quality Si-rich ore.

The use of LIBS for geological analysis was strongly stimulated by the introduction on the instrumentation market of portable and handheld LIBS instruments.[10,82,83] For example, Wang *et al.*[84] studied the elemental composition of stream sediments, an issue that could provide essential information about the geological evolution of a region, helping the reconstruction of the water environment in different geological periods. The laboratory analysis aimed at detecting and quantifying the presence of stromatolite phosphorite powder, which is a biomineral that easily enters in stream sediments due to weathering. The discovery of this material in extraterrestrial environments could thus shed light on the search for extraterrestrial life. The LIBS measurements were done in a vacuum chamber (no attempt was made to simulate the Martian environment), at a distance of 7 meters from the targets, and in a configuration similar to the LIBS instruments mounted on Martian rovers[85] (Fig. 5). A backpropagation artificial neural network (BP-ANN) was used to find and quantify, among other elements, phosphorus. The training set was formed by mixing stromatolite phosphorite powder with Yangtze River sediment (Wuhan), in different proportions, with phosphorus concentration ranging from 0.07 wt% to 1.3 wt%. A coefficient of determination $R^2 = 0.93$ with an RMSE = 0.1 wt% was achieved.

Recently, Mezoued *et al.*[86] published a data paper containing over 12 000 LIBS spectra from 170 pure mineral samples, acquired using a handheld LIBS analyzer. The paper includes LIBS spectra from, among others, various phosphates (*e.g.*, amblygonite, apatite, and topaz).

The reviewed studies clearly show that chemometric approaches have become an essential component of modern LIBS phosphorus analysis. Their effectiveness, however, strongly depends on the representativeness of the calibration datasets and on the capability of the models to account for matrix variability.

3.4 Industrial process monitoring and online LIBS analysis

In 2007, Gondal *et al.*[87] used LIBS for determining the concentration of hazardous metals in iron slag wastes collected from a local industry. Using a conventional calibration curve approach, the phosphorus concentration in the slag was found to be 2805 mg kg^{-1}, a value that was in good agreement with ICP-OES measurements.

Gaft *et al.*[88] realized an industrial LIBS machine for on-belt evaluation of phosphate by detecting Mg, Fe, Al, bone phosphate lime (BPL), insoluble phase and metal impurity ratio (MER). The instrument was also used for measuring the ash content in coal. The importance of online analysis of phosphate rock was remarked, as the presence of metallic pollutants may negatively affect the recovery of phosphate from the rock. The difficulty of performing quantitative analysis on trace elements on a moving conveyor belt was also discussed, stressing the need of fast and efficient methods for spectra selection and normalization.

Ahamer *et al.*[89] used a hybrid method for the analysis of oxides in steel slags. While the major oxide concentration was determined using CF-LIBS,[90] the concentration of minor P_2O_5 oxide was measured using a univariate calibration curve built using the 214.92 nm phosphorus line after normalization with the Si line at 390.55 nm. The reason for using different strategies for major and minor oxides is due to the poor precision of the CF-LIBS method in measuring low-concentration elements.[91,92] Moreover, the normalization of the phosphorus signal with the 390.55 silicon line reduced the effect of the ablated mass variation (both shot-to-shot and matrix-related), allowing for a good linearity of the calibration curve (R^2 = 0.998, with a LOD = 0.07 wt%).

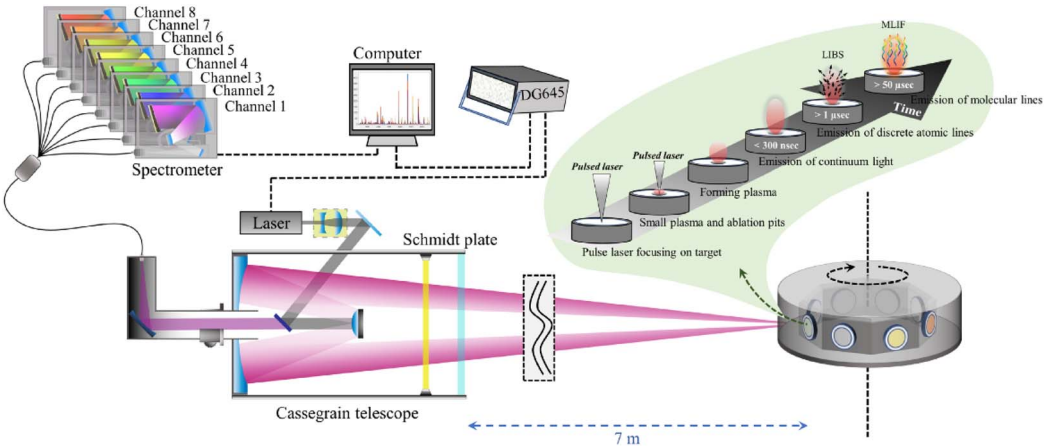

Fig. 5 Schematic representation of the experimental setup for the analysis of stream sediments. Figure reprinted from ref. 84 under Creative Commons CC BY license.

The analysis of phosphate ore slurries has also been undertaken by various authors (Rifai *et al.*, 2020; Dong *et al.*, 2021; Zhang *et al.*, 2024). Rifai *et al.* (2020)[93] analyzed phosphate powders, both slurries and pellets, from the production line using a commercial LIBS equipment. The estimated and reference concentrations showed a weak correlation (the coefficients of determination were less than 0.5) when using a univariate-based calibration model. Thus, in order to achieve a good correlation between the calculated and reference concentrations for P, Si, Mg, C, Fe, and Al, a chosen set of variables for an MLR model was tried, which resulted in R^2 values better than 0.96 and 0.99 for pressed pellets and slurries, respectively. Compared to pressed pellets, the predicted concentrations of the validation samples showed a lower bias relative error in slurries, probably because the slurries involved a better sampling and more representative larger mass of material. These findings demonstrate that direct LIBS measurements on slurry samples are a workable method for monitoring the phosphate ore extraction process.

In 2021, Dong *et al.*[94] introduced the use of CNN for determining the phosphorus content in the flotation process of phosphate ore slurries. The authors compared the results of different lightweight CNN structures to those obtained by PLS and SVM, finding that CNN predictions (RMSE = 0.89 wt%) were more accurate than the PLS ones (RMSE = 1.35 wt%), while PLS was more accurate than SVM (RMSE = 1.57 wt%). The authors concluded that lightweight CNN models might mitigate matrix effects and effectively improve the accuracy of prediction of P_2O_5 concentration in phosphate iron ore slurries.

Recently, Zhang *et al.* (2024)[95] used a self-developed on-line LIBS analyzer named LIBSlurry in a phosphate ore flotation plant in Yunnan Province, China. A method was proposed in which plasma images in two orthogonal directions were captured synchronously to describe the irregular plasma and used as the features. A spectral correction method based on these features was proposed to solve the problems of large signal fluctuations and poor measurement accuracy. As a result, the RSDs of the characteristic spectral intensity decreased from more than 20% to less than 3%, improving significantly the stability of spectra. Furthermore, the combination of the plasma image projection compensation (IPC) method and PLSR increased the R^2 for P_2O_5 to 0.99 and reduced the MAE of the test samples to less than 0.5%, so meeting the requirements of the phosphate rock flotation process.

Li *et al.* (2023)[96] determined total iron (TFe), silica (SiO_2), aluminum oxide (Al_2O_3), and phosphorus using an online LIBS system optimized for the determination of main components in the iron ore transported on belt conveyors at a speed of about 4 m s^{-1} performed at distance using a Maksutov-Cassegrain telescope. After the application of specific algorithms for LIBS signal normalization and baseline removal, a high accuracy was achieved, with RMSE = 0.0131% and ARE = 0.01% for phosphorus analysis in iron ore, at a working distance of 0.78 m.

Recent methodological developments demonstrate that improvements in instrumentation, signal enhancement techniques, and advanced data processing are progressively extending the analytical capabilities of LIBS for phosphorus determination. Nevertheless, further efforts are still required to improve robustness under real-world operating conditions.

3.5 Biomedical and diagnostic applications

At the beginning of the century, Pharmalaser Inc. introduced on the market a LIBS instrument for the analysis of pharmaceuticals, called PharmaLIBS 250.[97] One of the applications of this instrument was the analysis of phosphorus in pharmaceutical tablets for oral use [ref. 76, and references therein]. In this work, tablets with different loadings of a phosphorus-containing active agent were analyzed quantitatively based on a calibration curve built using the intensity of the unresolved P I doublet at 253.40 nm and 253.56 nm, normalized by the C I line at 247.86 nm. The authors warned about the fact that carbon is also contained in the active agent and, therefore, the normalization procedure would not be ideal but concluded that the ablated mass variations from shot-to-shot and from sample to sample were more problematic than the use of a less-than-perfect normalization. The overall quality of the resulting

calibration curve was considered satisfactory for the quantification task.

Gazmeh *et al.*[99] in 2015 used chemometric analysis (Partial Least Square-Discriminant Analysis, PLS-DA) for successfully discriminating carious from healthy teeth using information about the spectral emission of several atoms and ions, such as P, Ca, Mg, Zn, K, Sr, C, Na, H, and O.

Marín-Roldán *et al.*[100] studied the Ca/P ratio in bones and biocompatible materials used for prostheses, since this concentration ratio provides important information about the mechanical properties of these biomaterials. The authors used a CF-LIBS approach, reporting in a Saha–Boltzmann plot[101] neutral lines of phosphorus and neutral and ionic lines of Ca, Mg, and Sr for the determination of the electron temperature, and measured the electron number density from the Stark broadening of the H_α line at 656.27 nm.[102] The authors thus determined in a bone sample a calcium-to-phosphorus atomic ratio of 1.6 ± 0.4 at 500 ns delay time, not far from the Ca/P = 1.67 value of hydroxyapatite ($Ca_5(PO_4)_3(OH)$).

Khan *et al.*[103] used LIBS for the discrimination of melanoma in human tissue samples. In melanoma samples, the concentrations of potassium, sodium, magnesium calcium and phosphorus (measured through the P II line at 531.61 nm) were found to be systematically higher than in healthy tissues. The phosphorus line showed the highest intensity for malignancies. Through the applications of several machine learning algorithms, the authors obtained high discrimination rates between healthy and cancerous tissues, with ANN and PLS-DA achieving the best results with a correct discrimination rate of 100%.

Bali *et al.*[104] analyzed by LIBS fingernails from patients suffering from chronic kidney disease. A PLS-DA analysis evidenced a strong correlation between the concentration of some elements and the presence of the kidney illness. With respect to healthy individuals, Ca, P, Fe, and Zn levels were lower in ill patients, while Mg, Mn, Cu, K, and Si levels were comparably higher.

In a recent paper, Xie *et al.*[105] analyzed by LIBS 122 calcium-based urinary stones (some of them containing calcium phosphate) for determining their elemental composition. The authors found that phosphorus was mainly present in the form of apatite, which substitutes Ca^{2+}. Together with apatite, the Ca^{2+} ions can also be substituted by Mg^{2+} and Sr^{2+}, as demonstrated by the strong correlation between P, Mg, and Sr concentrations measured in the analyzed samples. Using ANN, a negative correlation was found between the intensity ratios of H, P, Mg, Sr, Na, and K over Ca with average stone density and a positive correlation with urine pH. Furthermore, the higher values of these ratios within the group of recurrent patients (patients who had previous occurrences of urine stones) was outlined, with respect to first-episode ones.

The studies reviewed in this section clearly demonstrate the wide applicability of LIBS for phosphorus determination in a broad range of matrices. At the same time, they also highlight several common challenges, including matrix effects, calibration transferability, spectral interferences, and the relatively weak analytical sensitivity of phosphorus emission lines. These limitations have stimulated the development of dedicated methodological approaches aimed at improving analytical performance. For this reason, the following section focuses on the principal strategies proposed to overcome these limitations and enhance the reliability of LIBS-based phosphorus quantification.

4. Discussion

4.1 What really limits phosphorus quantification in LIBS?

In this paper, we have presented and discussed the current experimental approaches and analytical methods developed in recent years for the determination of phosphorus concentration in complex matrices, such as fertilizers, soils, plants, and geological and industrial materials, using the LIBS technique. The discussed studies collectively show that phosphorus quantification by LIBS cannot be reduced to a simple comparison of calibration performances, since the analytical reliability strongly depends on matrix complexity, model assumptions, and validation strategy.

The evolution of the results obtained over the last decade for phosphorus quantification in different matrices clearly demonstrates the continuous improvement of the analytical performance achieved by LIBS, confirming the maturity of the technique as a rapid, precise, and environmentally friendly method for phosphorus analysis, both in laboratory and field applications. In many applications requiring quantitative determination of phosphorus content in different matrices, LIBS is now competitive with traditional laboratory-based analytical techniques.

From an experimental point of view, conventional laboratory setups are still employed in most applications, although the use of combined approaches (*e.g.*, LIBS + LIF, LIBS + digital imaging, *etc.*) is steadily increasing, thanks to the availability of robust data-fusion and data-analysis methods. Another important line of development for LIBS-based phosphorus analysis is represented by the growing diffusion of handheld LIBS instrumentation, which has opened new perspectives for *in situ* phosphorus analysis.

These recent developments, together with the well-known sensitivity of LIBS spectra to sample matrix effects, have stimulated the adoption of advanced spectral-analysis strategies aimed at improving robustness and transferability. The works discussed in Section 3 can therefore be grouped according to the quantification strategy adopted, as summarized in Table 2.

4.2 Univariate *vs.* multivariate approaches

From the analysis of the works reported in Table 2, it appears that, over the last decade, multivariate techniques have progressively replaced the conventional univariate approach based on calibration curves. The literature reveals that, in most cases, linear methods such as PLS regression are employed, whereas more complex nonlinear approaches based on artificial neural networks or deep-learning techniques, such as convolutional neural networks, remain relatively limited, although their use has proportionally increased in recent years.

Table 2 Works discussed in Section 3, grouped according to the main phosphorus quantification approach and application

Quantification approach	Works discussed	Specific application
Univariate calibration/line intensity, often with normalization	Marangoni *et al.*;[28] Nicolodelli *et al.*;[30] Vieira *et al.*;[37] Dib *et al.*;[38] Zhang *et al.*;[49] Ma and Dong;[54] Zhao *et al.*;[61] Steen *et al.*;[72] Gondal *et al.*;[87] Ahamer *et al.*;[89] St-Onge *et al.*[98]	Fertilizers; organic fertilizers; biochar-based fertilizers; water after liquid-to-solid conversion; pesticide residues on fruit/vegetables; cocoa-bean imaging; iron and steel slags; pharmaceutical tablets
Simple ratios and semiquantitative proxies	Asimellis *et al.*;[81] Rosenwasser *et al.*;[80] Steen *et al.*[72]	Phosphate ore grading; P/Si ratio in ores; elemental mapping of seeds
PLS/PLSR and related linear multivariate regression	Li *et al.*;[27] Senesi *et al.*;[33] Zhang *et al.*;[34] Xu *et al.*;[42] Sánchez-Esteva *et al.*;[46] Erler *et al.*;[48] Babos *et al.*;[57] Gamela *et al.*;[62] Tian *etal.*;[68] Martin *et al.*;[69] Sezer *etal.*;[70] Rifai *et al.*;[93] Zhang *et al.*[95]	Fertilizers; soils and soil P pools; mineral supplements; beans; seafood; switchgrass biomass; cheese; phosphate pellets/slurries; on-line slurry monitoring
Variable selection and sparse/alternative linear models	Sánchez-Esteva *et al.*;[46] Erler *et al.*[48]	Soil total P and extractable P pools; handheld LIBS analysis of agricultural soils
Nonlinear machine learning: SVM, ANN, BP-ANN, GPR	Sha *et al.*;[35] Zhang *et al.*;[49] Tian *et al.*;[69] Wang *et al.*;[84] Erler *et al.*;[48] Khan *et al.*;[103] Xie *et al.*[105]	Fertilizers; water residues; seafood; stream sediments containing phosphorite; topsoil and plant-available P; medical tissue and urinary stones
Deep learning/CNN	Xu *et al.*;[43] Massa *et al.*;[78] Dong *et al.*[94]	Soil total P and soil properties; sewage sludge ash; phosphate ore slurry flotation
Calibration-free LIBS and hybrid CF-LIBS	Aldakheel *et al.*;[63] Elsayed *et al.*;[77] Ahamer *et al.*;[89] Marin-Roldán *et al.*;[100] Ciucci *et al.*;[90] Tognoni *et al.*;[91] Poggialini *et al.*[92]	Moringa leaves; phosphogypsum; steel slags; bones and biocompatible materials; methodological CF-LIBS basis
Signal enhancement combined with calibration	Nicolodelli *et al.*;[30] Vieira *et al.*;[37] Dib *et al.*;[38] Soni *et al.*;[44,45] Zhao *et al.*[61]	Double-pulse LIBS for fertilizers; spark-assisted LIBS for fertilizers; LIBS-LIF for soils; nanoparticle-enhanced LIBS for pesticide residues
Data fusion and auxiliary information	Babos *et al.*;[39] Sánchez-Esteva *et al.*;[46] Gamela *et al.*;[63] Zhang *et al.*[95]	LIBS plus digital images for fertilizers; LIBS plus vis-NIRS for soil P pools; LIBS plus WD-XRF for beans; plasma imaging plus LIBS for slurries
Discrimination/classification using P-containing spectral features	Ma and Dong;[54] Senesi *et al.*;[33] Gazmeh *et al.*;[99] Khan *et al.*;[103] Bali *et al.*;[104] Nouman Khan *et al.*[71]	Pesticide detection; fertilizer discrimination; teeth, melanoma tissue, fingernails; medicinal plants

A closer examination of the studies summarized above shows that the use of increasingly sophisticated algorithms in LIBS analysis of phosphorus does not necessarily improve the quality of the analytical results unless both physical matrix effects, related, for example, to differences in ablated mass and particle size, and chemical matrix effects, associated with composition-dependent plasma excitation conditions, are explicitly considered.[9,20]

For this reason, the simplicity of univariate calibration methods may still remain attractive when the samples belong to a sufficiently narrow matrix class or when the analytical objective is process control rather than absolute traceable quantification. This is the case for relatively homogeneous fertilizers, tablets, steel slags, or controlled liquid-to-solid water residues, especially when a P line, frequently at 213.62, 214.91, or 253.56 nm, can be normalized to the continuum, carbon, silicon, or another matrix line.[19,28,29,40,74,84] Such procedures can reduce fluctuations due to ablated mass and instrumental drift, but they do not fully correct changes in plasma excitation conditions. Therefore, a univariate calibration built on one fertilizer family, one soil type, or one biological tissue cannot be assumed to be transferable to another family without validation on independent matrix-matched samples.

Multivariate calibration represents the most common practical solution adopted in the phosphorus-LIBS literature. PLS, MLR, Lasso, GPR, and related methods exploit several spectral variables simultaneously and can account, at least empirically, for matrix-induced changes in the analyte signal.[18,25,33,37–39,48,54–56,78,80] From an operational point of view, these methods can exploit the spectral fingerprints of Ca, Mg, Fe, Al, K, C, N, O, or Si, which are often chemically or physically linked to phosphorus in soils, plants, fertilizers, ashes, ores, and biological matrices. However, when the model uses variables that are not direct P emission lines, the prediction may reflect correlations present in the calibration set rather than genuine spectroscopic information related to phosphorus. In practice, this means that the model can perform very well in cross-validation, yet fails when the source, production process, soil horizon, organic matter content, moisture, mineralogy, or particle-size distribution changes.

4.3 Is machine learning really solving LIBS?

The above mentioned issue becomes even more relevant for machine-learning and deep-learning models that can describe nonlinear relations between spectra and reference concentrations. Several works report clear improvements over univariate

calibration and/or linear multivariate methods such as PLS, for example in fertilizers, seafood, stream sediments, phosphate slurries, and sewage sludge ash.[26,54,64,69,79]

However, the main risk of machine learning in LIBS is the construction of a chemically plausible yet analytically fragile black box. The problem is evident in studies where phosphorus is predicted even though the P emission lines are weak or not visible.[34,55] In such cases, the model may infer P concentration from Ca, Mg, Fe, K, organic matter, or other correlated variables. This can be useful for classification, screening, and prediction within a well-defined population of samples, but it should not be presented as a universal determination of phosphorus. If, for example, a soil amendment changes the Ca/P relationship, or a sewage sludge ash has a different mineralogical origin from those represented in the training set, a black-box model may return an apparently precise yet completely incorrect value. For this reason, external validation on independent datasets, together with explicit reporting of the selected spectral regions, is more important than the nominal complexity of the algorithm.

The paper by Massa *et al.* on sewage sludge ash is particularly instructive in this respect: real SSA samples, independently characterized, were used during model validation and optimization, forcing the CNN to learn spectral features that remained useful under realistic matrix variability.[78] This approach is closer to real analytical practice than the development of a high-performing model on a narrow training set followed by validation on samples drawn from the same distribution.

A practical criterion for evaluating machine-learning models in LIBS is whether they remain interpretable at the spectroscopic level. Useful models should either include P lines among the influential variables or provide a clear chemical explanation for the indirect variables used. Variable-selection methods such as CARS, iPLS, Lasso, and imaging-assisted correction are valuable because they reduce model complexity and help identify whether the prediction is driven by P emission, matrix descriptors, or accidental correlations.[37–39,80] Similarly, data fusion with digital imaging, vis-NIRS, WD-XRF, or plasma imaging can improve robustness when the added information describes real sources of variability, such as sample texture, organic matter, mineralogy, or shot-to-shot plasma geometry.[30,37,48,80]

4.4 Calibration-free LIBS: promises and limitations

Calibration-free LIBS offers a conceptually different approach. Instead of learning a sample-specific calibration, CF-LIBS attempts to reconstruct the elemental composition from plasma physics by measuring the line intensities and the electron temperature and number density of the laser-induced plasma.[75,76] This is attractive for phosphorus analysis because, in principle, it should suppress matrix effects while eliminating dependence on reference standards. In practice, however, its reliability depends on demanding conditions: the plasma must be observed within a time window in which temperature and density are well defined, ensuring that the plasma is close to LTE and optically thin, or that self-absorption is correctly treated.[52,53,75–77] These requirements explain why CF-LIBS is more appropriate for laboratory studies, major-element analysis, or well-controlled samples than for field measurements on heterogeneous soils, slurries, or biological materials.

For phosphorus, the limitations of CF-LIBS are particularly evident. When P is present as a minor element, the weak UV lines may provide insufficient information for robust treatment, and small errors in the measured line intensities or in the spectroscopic parameters may produce large concentration errors.[76,77] The works on Moringa leaves, phosphogypsum, bones, and steel slags illustrate both the promise of the technique and the caution required in its application.[49,63,74,86] In steel slags, a hybrid strategy proved more realistic: CF-LIBS was used for major oxides, whereas P_2O_5 was quantified through a normalized univariate calibration.[74] This confirms a practical conclusion already present in the CF-LIBS literature: calibration-free procedures are powerful, but they are not automatically superior to calibrated methods for minor elements.[52,75–77]

In any case, it appears clear that the most successful studies combine an appropriate physical protocol with an analytical model whose assumptions are consistent with the analytical task. Normalization can compensate for shot-to-shot variability; PLS or MLR can partially correct for matrix variation; SVM, ANN, and CNN can model nonlinearities; and CF-LIBS can provide standard-free insight under controlled plasma conditions. None of these approaches, however, eliminates the need for representative samples and independent validation.

4.5 Practical considerations and future directions

In real practice, the best quantification strategy is therefore application-dependent. For quality control of a single production line, such as phosphate slurry flotation or conveyor-belt ore monitoring, a multivariate or deep-learning model trained on representative process samples may be the most efficient solution, especially if coupled with normalization, plasma imaging, or spectral refinement.[78–82] For regulatory or inter-laboratory measurements on heterogeneous soils, fertilizers, ashes, or foods, the model should be validated across independent sources and should include uncertainty estimates, matrix-class diagnostics, and warning rules for samples lying outside the calibration domain. For exploratory field screening, handheld LIBS can provide rapid classification and approximate quantification of P, but confirmatory analysis may still require laboratory reference methods or matrix-matched calibration.

Another important point concerns the role of sample preparation. Pelleting, drying, grinding, liquid-to-solid conversion, and controlled blending with standards may appear to reduce the immediacy of LIBS, but in many cases they are necessary to obtain meaningful analytical results.

5. Conclusion

In conclusion, the most convincing phosphorus-LIBS applications are those in which the model structure, the calibration design, and the sample population are fully consistent with the

analytical question. Conversely, models that predict phosphorus from hidden correlations in small or homogeneous datasets may provide an unrealistic impression of accuracy. Future work should therefore focus not only on the analytical results obtained, but also on their statistical validity and their ability to generalize to independent datasets. To this end, accurate specification of the selected wavelengths or features, the matrix range covered by calibration and validation, and the behavior of the model when P lines are weak, absent, or perturbed will be essential.

Author contributions

V. P.: work conception and design, literature analysis, manuscript draft and figures realization. G. S. S., S. L., G. L., F. P., B. C., S. D. I., L. E. D., L. B., E. B.: literature analysis, manuscript revision. The manuscript was written through the contributions of all the authors. All authors have read and agreed to the published version of the manuscript.

Conflicts of interest

The authors declare no conflicts of interest.

Abbreviations

ANN	Artificial neural network
AP	Available phosphorus
BP-ANN	Backpropagation artificial neural network
BPL	Bone phosphate lime
CF-LIBS	Calibration-free LIBS
CNN	Convolutional neural network
CRM	Critical raw materials
DIMP	Diisopropylmethyl phosphonate
DL	Deep learning
EU	European Union
ICP-OES	Inductively-coupled plasma optical emission spectroscopy
LIBS	Laser-induced breakdown spectroscopy
LIF	Laser-induced fluorescence
LOD	Limit of detection
MAE	Mean absolute error
MAPE	Mean absolute percentage error
MEC	Multi-energy calibration
MER	Metal impurity ratio
MSE	Mean squared error
NIST	National Institute of Standards and Technology
OP GSA	One-point gravimetric standard addition
PLS	Partial least squares
PLS-DA	Partial least square-discriminant analysis
PMM-MEC	Partial matrix matching multi-energy calibration
REP	Relative error of prediction
RMSE	Root mean square error
RSD	Relative standard deviation
SOM	Solid organic matter
SSA	Sewage sludge ash
SVM	Support vector machine
TK	Total potassium
TFe	Total iron
TN	Total nitrogen
TP	Total phosphorus
USA	United States of America
USD	US dollars
UV	Ultraviolet
WD-XRF	Wavelength-dispersive X-ray fluorescence
XPS	X-ray photoelectron spectroscopy
XRF	X-ray fluorescence

Data availability

Data are contained within the article.

Acknowledgements

This work was supported by F.O.S.F.O.R.O. (Fanghi Organici Sostenibili per il Futuro: Ottimizzazione del Recupero di Ortofosfati e altri nutrienti, CUP: E89I25001040007), co-financed by Regione Lombardia, the European Union, and ERDF. The graphical abstract was realized by using Biorender. The author used ChatGPT 5.2 for orthographic and grammatical correction of the text. The authors have reviewed and edited the output and take full responsibility for the content of this publication.

References

1 European Parliament and Council of the European Union, *Regulation (EU) 2024/1252 of the European Parliament and of the Council of 11 April 2024 establishing a framework for ensuring a secure and sustainable supply of critical raw materials and amending regulations (EU) no. 168/2013, (EU) 2018/858, (EU) 2018/1724 and (EU) 2019/1020*, Official Journal of the European Union L, 2024, https://eur-lex.europa.eu/eli/reg/2024/1252/oj, accessed July 11, 2026.

2 U.S. Geological Survey, *Mineral Commodity Summaries 2025: Phosphate Rock*, https://pubs.usgs.gov/publication/mcs2025, accessed July 11, 2026.

3 International Fertilizer Association (IFA), *Fertilizer Consumption 1961–2023*, 2025, https://ifastat.org/fertilizer-reports-analysis/fertilizer-consumption, accessed July 11, 2026.

4 H. Diskowski and T. Hofmann, Phosphorus, in *Ullmann's Encyclopedia of Industrial Chemistry*, Wiley, 2000, DOI: 10.1002/14356007.a19_505.

5 D. Cordell, J. O. Drangert and S. White, The story of phosphorus: Global food security and food for thought, *Glob. Environ. Change*, 2009, **19**, 292–305, DOI: 10.1016/J.GLOENVCHA.2008.10.009.

6 J. Elser and E. Bennett, A broken biogeochemical cycle, *Nature*, 2011, **478**(7367), 29–31, DOI: 10.1038/478029a.

7 *Phosphorus & Derivatives Market Size, Share, Trends & Forecast*, https://www.verifiedmarketreports.com/product/

phosphorus-and-derivatives-market/?utm_source=chatgpt.com/, accessed July 11, 2026.
8 M. Massa, E. Galli, A. Zanoletti, A. Zacco, S. De Iuliis, L. E. Depero, V. Palleschi, L. Borgese and E. Bontempi, Overcoming matrix effects on the determination of phosphorus concentration in sewage sludge ash using laser-induced breakdown spectroscopy hand-held instrumentation, *Spectrochim. Acta, Part B*, 2026, **235**, 107377, DOI: 10.1016/J.SAB.2025.107377.
9 V. Palleschi, Laser-induced breakdown spectroscopy: principles of the technique and future trends, *ChemTexts*, 2020, **6**, 18, DOI: 10.1007/s40828-020-00114-x.
10 G. S. Senesi, R. S. Harmon and R. R. Hark, Field-portable and handheld laser-induced breakdown spectroscopy: historical review, current status and future prospects, *Spectrochim. Acta, Part B*, 2021, **175**, 106013, DOI: 10.1016/J.SAB.2020.106013.
11 T. R. Loree and L. J. Radziemski, Laser-induced breakdown spectroscopy: time-integrated applications, *Plasma Chem. Plasma Process.*, 1981, **1**, 271–279, DOI: 10.1007/BF00568835.
12 L. J. Radziemski and T. R. Loree, Laser-induced breakdown spectroscopy: time-resolved spectrochemical applications, *Plasma Chem. Plasma Process.*, 1981, **1**, 281–293, DOI: 10.1007/BF00568836.
13 M. Milán, P. Lucena, L. M. Cabalín and J. J. Laserna, Depth profiling of phosphorus in photonic-grade silicon using laser-induced breakdown spectrometry, *Appl. Spectrosc.*, 1998, **52**, 444–448, DOI: 10.1366/0003702981943662.
14 M. Corsi, V. Palleschi and E. Tognoni, Special Issue – LIBS2000 – 1st International Conference on Laser Induced Plasma Spectroscopy and Applications - Preface, *Spectrochim. Acta, Part B*, 2001, **56**, 565–566.
15 Q. Yuan, W. Sheng, Z. Zhang, H. Li and M. Zhang, Recent Advances in Soil Nutrient Monitoring: A Review, in *Smart Agriculture*, Springer, Singapore, 2023, pp. 19–38, DOI: 10.1007/978-981-99-7927-1_2.
16 G. S. Senesi, Laser-Induced Breakdown Spectroscopy (LIBS) applied to terrestrial and extraterrestrial analogue geomaterials with emphasis to minerals and rocks, *Earth-Sci. Rev.*, 2014, 231–267, DOI: 10.1016/J.EARSCIREV.2014.09.008.
17 V. Palleschi, S. Legnaioli, F. Poggialini, F. O. Bredice, I. A. Urbina, N. Lellouche and S. M. Aberkane, Laser-induced breakdown spectroscopy, *Nat. Rev. Methods Primers*, 2025, **5**, 1–16, DOI: 10.1038/S43586-025-00388-W.
18 S. Legnaioli, A. Botto, B. Campanella, F. Poggialini, S. Raneri and V. Palleschi, *Univariate Linear Methods*, John Wiley & Sons, Ltd, 2022, DOI: 10.1002/9781119759614.CH11.
19 A. Safi, B. Campanella, E. Grifoni, S. Legnaioli, G. Lorenzetti, S. Pagnotta, F. Poggialini, L. Ripoll-Seguer, M. Hidalgo and V. Palleschi, Multivariate calibration in Laser-Induced Breakdown Spectroscopy quantitative analysis: the dangers of a 'black box' approach and how to avoid them, *Spectrochim. Acta, Part B*, 2018, **144**, 46–54, DOI: 10.1016/J.SAB.2018.03.007.
20 NIST, *NIST: Atomic Spectra Database Lines Form*, https://physics.nist.gov/PhysRefData/ASD/lines_form.html, accessed April 29, 2020.
21 A. Kramida, K. Olsen and Y. Ralchemko, *NIST LIBS Database*, https://physics.nist.gov/PhysRefData/ASD/LIBS/libs-form.html, accessed December 10, 2025.
22 IUPAC, Nomenclature, symbols, units and their usage in spectrochemical analysis—II. data interpretation analytical chemistry division, *Spectrochim. Acta, Part B*, 1978, **33**, 241–245, DOI: 10.1016/0584-8547(78)80044-5.
23 F. Poggialini, S. Legnaioli, B. Campanella, B. Cocciaro, G. Lorenzetti, S. Raneri and V. Palleschi, Calculating the Limits of Detection in Laser-Induced Breakdown Spectroscopy: Not as Easy as It Might Seem, *Appl. Sci.*, 2023, **13**, 3642, DOI: 10.3390/APP13063642.
24 M. Otto, *Chemometrics*, Wiley, Weinheim (Germany), 2016, DOI: 10.1002/9783527699377.
25 G. Nicolodelli, J. Cabral, C. R. Menegatti, B. Marangoni and G. S. Senesi, Recent advances and future trends in LIBS applications to agricultural materials and their food derivatives: an overview of developments in the last decade (2010–2019). Part I. Soils and fertilizers, *TrAC, Trends Anal. Chem.*, 2019, **115**, 70–82, DOI: 10.1016/j.trac.2019.03.032.
26 G. S. Senesi, J. Cabral, C. R. Menegatti, B. Marangoni and G. Nicolodelli, Recent advances and future trends in LIBS applications to agricultural materials and their food derivatives: an overview of developments in the last decade (2010–2019). Part II. Crop plants and their food derivatives, *TrAC, Trends Anal. Chem.*, 2019, **118**, 453–469, DOI: 10.1016/j.trac.2019.05.052.
27 J. Li, S. Yao, J. Lu, J. Li, K. Chen and M. Dong, Multi-elemental analysis of fertilizer using laser-induced breakdown spectroscopy coupled with partial least squares regression, *J. Anal. At. Spectrom.*, 2010, **25**, 1733–1738, DOI: 10.1039/c0ja00027b.
28 B. S. Marangoni, K. S. G. Silva, G. Nicolodelli, G. S. Senesi, J. S. Cabral, P. R. Villas-Boas, C. S. Silva, P. C. Teixeira, A. A. Rita Nogueira, V. M. Benites and D. M. B. P. Milori, Phosphorus quantification in fertilizers using laser induced breakdown spectroscopy (LIBS): a methodology of analysis to correct physical matrix effects, *Anal. Methods*, 2016, **8**(1), 78–82, DOI: 10.1039/c5ay01615k.
29 S. Sánchez-Esteva, M. Knadel, R. Labouriau, G. H. Rubæk and G. Heckrath, Total Phosphorus Determination in Soils Using Laser-Induced Breakdown Spectroscopy: Evaluating Different Sources of Matrix Effects, *Appl. Spectrosc.*, 2021, **75**, 22–33, DOI: 10.1177/0003702820949560.
30 G. Nicolodelli, G. S. Senesi, I. L. de Oliveira Perazzoli, B. S. Marangoni, V. De Melo Benites and D. M. B. P. Milori, Double pulse laser induced breakdown spectroscopy: a potential tool for the analysis of contaminants and macro/micronutrients in organic mineral fertilizers, *Sci. Total Environ.*, 2016, **565**, 1116–1123, DOI: 10.1016/J.SCITOTENV.2016.05.153.

31 G. Cristoforetti and V. Palleschi, *Double-pulse Laser Ablation of Solid Targets in Ambient Gas: Mechanisms and Effects*, Nova Science Publishers, Inc., 2011.

32 G. C. Y. Chan, G. M. Hieftje, N. Omenetto, O. Axner, A. Bengtson, N. H. Bings, M. W. Blades, A. Bogaerts, M. A. Bolshov, J. A. C. Broekaert, W. T. Chan, J. M. Costa-Fernández, S. R. Crouch, A. De Giacomo, A. D'Ulivo, C. Engelhard, H. Falk, P. B. Farnsworth, S. Florek, G. Gamez, I. B. Gornushkin, D. Günther, D. W. Hahn, W. Hang, V. Hoffmann, N. Jakubowski, V. Karanassios, D. W. Koppenaal, R. K. Marcus, R. Noll, J. W. Olesik, V. Palleschi, U. Panne, J. Pisonero, S. J. Ray, M. Resano, R. E. Russo, A. Scheeline, B. W. Smith, R. E. Sturgeon, J. L. Todolí, E. Tognoni, F. Vanhaecke, M. R. Webb, J. D. Winefordner, L. Yang, J. Yu and Z. Zhang, Landmark Publications in Analytical Atomic Spectrometry: Fundamentals and Instrumentation Development, *Appl. Spectrosc.*, 2025, **79**, 481–735, DOI: 10.1177/00037028241263567.

33 G. S. Senesi, R. A. Romano, B. S. Marangoni, G. Nicolodelli, P. R. Villas-Boas, V. M. Benites and D. M. B. P. Milori, Laser-Induced Breakdown Spectroscopy Associated with Multivariate Analysis Applied to Discriminate Fertilizers of Different Nature, *J. Appl. Spectrosc.*, 2017, **84**, 923–928, DOI: 10.1007/s10812-017-0566-4.

34 B. Zhang, P. Ling, W. Sha, Y. Jiang and Z. Cui, Univariate and multivariate analysis of phosphorus element in fertilizers using laser-induced breakdown spectroscopy, *Sensors*, 2019, **19**, 1727, DOI: 10.3390/s19071727.

35 W. Sha, J. Li, W. Xiao, P. Ling and C. Lu, Quantitative analysis of elements in fertilizer using laser-induced breakdown spectroscopy coupled with support vector regression model, *Sensors*, 2019, **19**, 3277, DOI: 10.3390/s19153277.

36 V. Palleschi, *Chemometrics and Numerical Methods in LIBS*, John Wiley, 2022.

37 A. L. Vieira, T. V. Silva, F. S. I. de Sousa, G. S. Senesi, D. S. Júnior, E. C. Ferreira and J. A. G. Neto, Determinations of phosphorus in fertilizers by spark discharge-assisted laser-induced breakdown spectroscopy, *Microchem. J.*, 2018, **139**, 322–326, DOI: 10.1016/J.MICROC.2018.03.011.

38 S. R. Dib, G. S. Senesi, J. A. G. Neto, C. A. Ribeiro and E. C. Ferreira, Phosphorous Determination in Biochar-Based Fertilizers by Spark Discharge-Laser-Induced Breakdown Spectroscopy, *Chemosensors*, 2021, **9**, 9, DOI: 10.3390/CHEMOSENSORS9120337.

39 D. V. Babos, J. F. K. Ramos, G. C. Francisco, V. d. M. Benites and D. M. B. P. Milori, Laser-induced breakdown spectroscopy and digital image data fusion for determination of the Al, Ca, Fe, Mg, and P in mineral fertilizer: overcome matrix effects in solid direct analysis, *J. Opt. Soc. Am. B*, 2023, **40**(3), 654–660, DOI: 10.1364/JOSAB.482619.

40 X. Zhong, F. Ma, J. Zhou and C. Du, Rapid fertilizer nutrient analysis enabled by handheld LIBS (hLIBS) and an intelligent Euclidean distance prediction algorithm, *Talanta*, 2026, **299**, 129120, DOI: 10.1016/j.talanta.2025.129120.

41 C. L. Cuiping Lu, L. W. Liusan Wang, H. H. Haiying Hu, Z. Z. Zhong Zhuang, Y. W. Yubing Wang, R. W. Rujing Wang and L. S. Liangtu Song, Analysis of total nitrogen and total phosphorus in soil using laser-induced breakdown spectroscopy, *Chin. Opt. Lett.*, 2013, **11**, 053004–053007, DOI: 10.3788/col201311.053004.

42 X. Xu, C. Du, F. Ma, Y. Shen and J. Zhou, Fast and simultaneous determination of soil properties using laser-induced breakdown spectroscopy (Libs): a case study of typical farmland soils in china, *Soil Syst.*, 2019, **3**, 66, DOI: 10.3390/soilsystems3040066.

43 X. Xu, F. Ma, J. Zhou and C. Du, Applying convolutional neural networks (CNN) for end-to-end soil analysis based on laser-induced breakdown spectroscopy (LIBS) with less spectral preprocessing, *Comput. Electron. Agric.*, 2022, **199**, 107171, DOI: 10.1016/j.compag.2022.107171.

44 S. Soni, J. Viljanen, R. Uusitalo and P. Veis, Phosphorus quantification in soil using LIBS assisted by laser-induced fluorescence, *Heliyon*, 2023, **9**, e17523, DOI: 10.1016/j.heliyon.2023.e17523.

45 S. Soni, J. Viljanen, R. Uusitalo and P. Veis, Total Soil Phosphorus Detection Using Laser-Induced Fluorescence-Assisted Laser-Induced Breakdown Spectroscopy, *Applied Industrial Spectroscopy in Proceedings Optica Sensing Congress 2023 (AIS, FTS, HISE, Sensors, ES)*, 2023, DOI: DOI: 10.1364/AIS.2023.AM2A.3.

46 S. Sánchez-Esteva, M. Knadel, S. Kucheryavskiy, L. W. de Jonge, G. H. Rubæk, C. Hermansen and G. Heckrath, Combining laser-induced breakdown spectroscopy (LIBS) and visible near-infrared spectroscopy (vis-NIRS) for soil phosphorus determination, *Sensors*, 2020, **20**, 5419, DOI: 10.3390/s20185419.

47 H. M. Al-Juboori, S. Z. H. Rizvi, J. Y. C. Liew and M. S. B. Roslan, Integrating Laser-Induced Breakdown Spectroscopy (LIBS) and Machine Learning for Soil Elemental Analysis: Exploring Atomic Interactions and Environmental Applications, *2025 IEEE International Conference on Automatic Control and Intelligent Systems, I2CACIS 2025 - Proceedings*, 2025, pp. 25–30, DOI: 10.1109/I2CACIS65476.2025.11100930.

48 A. Erler, D. Riebe, T. Beitz, H.-G. Löhmannsröben and R. Gebbers, Soil Nutrient Detection for Precision Agriculture Using Handheld Laser-Induced Breakdown Spectroscopy (LIBS) and Multivariate Regression Methods (PLSR, Lasso and GPR), *Sensors*, 2020, **20**, 418, DOI: 10.3390/S20020418.

49 H. Zhang, Y. Chen, Z. Bi, X. Che, Z. Tian, H. Zhang, Y. Chen, Z. Bi, X. Che and Z. Tian, Detection of Phosphorus in Water by Laser-Induced Breakdown Spectroscopy Based on Liquid-Solid Transformation of Graphite Substrate Combined with PLS-SVR Fusion Quantitative Analysis Algorithm, *Photonics*, 2025, **12**, 12, DOI: 10.3390/PHOTONICS12060616.

50 X. Yang, X. Wang, X. Wang, B. Wang, D. Li, X. Zhang, H. Ren, Z. Qin, Z. Zhou and X. Zheng, Detection of trace

phosphorus in water by plasma amplification laser-induced breakdown spectroscopy, *Opt. Express*, 2023, **31**, 40345, DOI: 10.1364/OE.502894.

51 X. Yang, X. Wang, D. Li, X. Zhang, K. Li, H. Ren, Z. Zhou, Z. Qin and X. Zheng, Effect of liquid aerosol temperature on the detection performance of LIBS for analysis of phosphorus element in water, *J. Anal. At. Spectrom.*, 2024, **39**, 433–438, DOI: 10.1039/d3ja00286a.

52 X. Yang, X. Wang, P. Zhu, F. Han, H. Ren, Z. Hua, Z. Qin, Z. Sun and X. Zheng, Detection of nitrogen in water by plasma amplification LIBS assisted with spatially resolved spectroscopy, *J. Anal. At. Spectrom.*, 2025, **40**, 1804–1809, DOI: 10.1039/d5ja00012b.

53 X. Yang, P. Zhu, D. Li, C. Liu, X. Zhang, T. Hong, H. Ren, Z. Hua, Z. Qin, Z. Sun and X. Zheng, Reducing laser energy to suppress air interference for plasma amplification LIBS detection of nitrogen in an aerosol solution, *J. Anal. At. Spectrom.*, 2025, **40**, 498–502, DOI: 10.1039/d4ja00325j.

54 F. Ma and D. Dong, A Measurement Method on Pesticide Residues of Apple Surface Based on Laser-Induced Breakdown Spectroscopy, *Food Anal. Methods*, 2014, **7**(9), 1858–1865, DOI: 10.1007/S12161-014-9828-4.

55 K. Devey, M. Mucalo, G. Rajendram and J. Lane, Pasture Vegetation Elemental Analysis by Laser-Induced Breakdown Spectroscopy, *Commun. Soil Sci. Plant Anal.*, 2015, **46**, 72–80, DOI: 10.1080/00103624.2014.988578.

56 G. G. Arantes de Carvalho, J. Moros, D. Santos, F. J. Krug and J. J. Laserna, Direct determination of the nutrient profile in plant materials by femtosecond laser-induced breakdown spectroscopy, *Anal. Chim. Acta*, 2015, **876**, 26–38, DOI: 10.1016/j.aca.2015.03.018.

57 D. V. Babos, A. I. Barros, J. A. Nóbrega and E. R. Pereira-Filho, Calibration strategies to overcome matrix effects in laser-induced breakdown spectroscopy: direct calcium and phosphorus determination in solid mineral supplements, *Spectrochim. Acta, Part B*, 2019, **155**, 90–98, DOI: 10.1016/j.sab.2019.03.010.

58 D. V. Babos, A. Virgilio, V. C. Costa, G. L. Donati and E. R. Pereira-Filho, Multi-energy calibration (MEC) applied to laser-induced breakdown spectroscopy (LIBS), *J. Anal. At. Spectrom.*, 2018, **33**, 1753–1762, DOI: 10.1039/C8JA00109J.

59 V. Costa, D. Babos, J. Castro, D. Andrade, R. Gamela, R. Machado, M. Sperança, A. Araújo, J. Garcia and E. Pereira-Filho, Calibration Strategies Applied to Laser-Induced Breakdown Spectroscopy: A Critical Review of Advances and Challenges, *J. Braz. Chem. Soc.*, 2020, **31**(12), 2439–2451, DOI: 10.21577/0103-5053.20200175.

60 X. Yang, D. Li, W. Ye, T. Hong, Z. Hua, Z. Qin and X. Zheng, Research Progress of Standard Addition Method Based on Laser-Induced Breakdown Spectroscopy, *Laser Technol.*, 2025, **49**, 403–411, DOI: 10.7510/jgjs.issn.1001-3806.2025.03.013.

61 X. Zhao, C. Zhao, X. Du and D. Dong, Detecting and Mapping Harmful Chemicals in Fruit and Vegetables Using Nanoparticle-Enhanced Laser-Induced Breakdown Spectroscopy, *Sci. Rep.*, 2019, **9**(1), 906, DOI: 10.1038/s41598-018-37556-w.

62 R. R. Gamela, V. C. Costa, M. A. Sperança and E. R. Pereira-Filho, Laser-induced breakdown spectroscopy (LIBS) and wavelength dispersive X-ray fluorescence (WDXRF) data fusion to predict the concentration of K, Mg and P in bean seed samples, *Food Res. Int.*, 2020, **132**, 109037, DOI: 10.1016/j.foodres.2020.109037.

63 R. K. Aldakheel, M. A. Gondal, M. M. Nasr, M. A. Almessiere and N. Idris, Spectral analysis of Miracle Moringa tree leaves using X-ray photoelectron, laser induced breakdown and inductively coupled plasma -optical emission spectroscopic techniques, *Talanta*, 2020, **217**, 121062, DOI: 10.1016/J.TALANTA.2020.121062.

64 D. A. Cremers and L. J. Radziemski, *Handbook of Laser-Induced Breakdown Spectroscopy*, John Wiley & Sons, Ltd, Chichester, UK, 2006, DOI: 10.1002/0470093013.

65 H. R. Griem, Stark Broadening, *Advances in Atomic and Molecular Physics*, 1976, vol. 11, pp. 331–359, DOI: 10.1016/S0065-2199(08)60033-0.

66 V. Palleschi, Seven Common Errors to Avoid in LIBS Analysis, *Spectroscopy*, 2019, **34**, 16–17.

67 G. Cristoforetti, A. De Giacomo, M. Dell'Aglio, S. Legnaioli, E. Tognoni, V. Palleschi and N. Omenetto, Local Thermodynamic Equilibrium in Laser-Induced Breakdown Spectroscopy: Beyond the McWhirter criterion, *Spectrochim. Acta, Part B*, 2010, **65**, 86–95, DOI: 10.1016/j.sab.2009.11.005.

68 Y. Tian, Q. Chen, Y. Lin, Y. Lu, Y. Li and H. Lin, Quantitative determination of phosphorus in seafood using laser-induced breakdown spectroscopy combined with machine learning, *Spectrochim. Acta, Part B*, 2021, **175**, 106027, DOI: 10.1016/J.SAB.2020.106027.

69 M. Martin, D. Brice, S. Martin, N. André and N. Labbé, Inorganic characterization of switchgrass biomass using laser-induced breakdown spectroscopy, *Spectrochim. Acta, Part B*, 2021, **186**, 106323, DOI: 10.1016/J.SAB.2021.106323.

70 B. Sezer, M. Ozturk, H. Ayvaz, H. Apaydın and I. H. Boyaci, Laser-induced breakdown spectroscopy as a reliable analytical method for classifying commercial cheese samples based on their cooking/stretching process, *Food Chem.*, 2022, **390**, 132946, DOI: 10.1016/J.FOODCHEM.2022.132946.

71 M. Nouman Khan, Q. Wang, B. S. Idrees, R. Waheed, A. U. Haq, M. Abrar and Y. Jamil, Evaluation of medicinal plants using laser-induced breakdown spectroscopy (LIBS) combined with chemometric techniques, *Laser Med. Sci.*, 2023, **38**(1), 149, DOI: 10.1007/S10103-023-03805-2.

72 T. Steen, F. Förste, D. Kadow, I. Mantouvalou, C. Keil and V. Merk, Elemental mapping of cocoa beans with laser-induced breakdown spectroscopy, *J. Trace Elem. Med. Biol.*, 2025, **90**, 127690, DOI: 10.1016/j.jtemb.2025.127690.

73 L. Jolivet, M. Leprince, S. Moncayo, L. Sorbier, C.-P. Lienemann and V. Motto-Ros, Review of the recent advances and applications of LIBS-based imaging, *Spectrochim. Acta, Part B*, 2019, **151**, 41–53, DOI: 10.1016/J.SAB.2018.11.008.

74 C. Fabre, D. Devismes, S. Moncayo, F. Pelascini, F. Trichard, A. Lecomte, B. Bousquet, J. Cauzid and V. Motto-Ros, Elemental imaging by laser-induced breakdown spectroscopy for the geological characterization of minerals, *J. Anal. At. Spectrom.*, 2018, **33**, 1345–1353, DOI: 10.1039/C8JA00048D.

75 L. Sancey, V. Motto-Ros, B. Busser, S. Kotb, J. M. Benoit, A. Piednoir, F. Lux, O. Tillement, G. Panczer and J. Yu, Laser spectrometry for multi-elemental imaging of biological tissues, *Sci. Rep.*, 2014, **4**, 6065, DOI: 10.1038/srep06065.

76 B. Busser, S. Moncayo, J. L. Coll, L. Sancey and V. Motto-Ros, Elemental imaging using laser-induced breakdown spectroscopy: a new and promising approach for biological and medical applications, *Coord. Chem. Rev.*, 2018, **358**, 70–79, DOI: 10.1016/J.CCR.2017.12.006.

77 K. Elsayed, W. Tawfik, A. E. M. Khater, T. S. Kayed and M. Fikry, Fast determination of phosphorus concentration in phosphogypsum waste using calibration-free LIBS in air and helium, *Opt. Quantum Electron.*, 2022, **54**, 1–14, DOI: 10.1007/S11082-021-03474-X.

78 M. Massa, E. Galli, A. Zanoletti, A. Zacco, S. De Iuliis, L. E. Depero, V. Palleschi, L. Borgese and E. Bontempi, Overcoming matrix effects on the determination of phosphorus concentration in sewage sludge ash using laser-induced breakdown spectroscopy hand-held instrumentation, *Spectrochim. Acta, Part B*, 2026, **235**, 107377, DOI: 10.1016/J.SAB.2025.107377.

79 E. Képeš, P. Pořízka and J. Kaiser, On the application of bootstrapping to laser-induced breakdown spectroscopy data, *J. Anal. At. Spectrom.*, 2019, **34**, 2411–2419, DOI: 10.1039/C9JA00304E.

80 S. Rosenwasser, G. Asimellis, B. Bromley, R. Hazlett, J. Martin, T. Pearce and A. Zigler, Development of a method for automated quantitative analysis of ores using LIBS, *Spectrochim. Acta, Part B*, 2001, **56**, 707–714, DOI: 10.1016/S0584-8547(01)00191-4.

81 G. Asimellis, A. Giannoudakos and M. Kompitsas, Phosphate ore beneficiation via determination of phosphorus-to-silica ratios by Laser Induced Breakdown Spectroscopy, *Spectrochim. Acta, Part B*, 2006, **61**, 1253–1259, DOI: 10.1016/j.sab.2006.10.011.

82 G. S. Senesi, Portable Hand Held Laser-induced Breakdown Spectroscopy (LIBS) Instrumentation for in-field Elemental Analysis of Geological Samples, *Int. J. Earth Environ. Sci.*, 2017, **2017**, 146, DOI: 10.15344/2456-351X/2017/146.

83 R. S. Harmon and G. S. Senesi, Laser-Induced Breakdown Spectroscopy – a geochemical tool for the 21st century, *Appl. Geochem.*, 2021, **128**, 104929, DOI: 10.1016/J.APGEOCHEM.2021.104929.

84 H. Wang, X. Yan, Y. Xin, P. Fang, Y. Wang, S. Liu, J. Jia, L. Zhang, X. Wan, H. Wang, X. Yan, Y. Xin, P. Fang, Y. Wang, S. Liu, J. Jia, L. Zhang and X. Wan, Determination of Elemental Composition and Content in Stream Sediments by Laser-Induced Breakdown Spectroscopy, *Chemosensors*, 2023, **11**, 11, DOI: 10.3390/CHEMOSENSORS11070377.

85 X. Wan, C. Li, H. Wang, W. Xu, J. Jia, Y. Xin, H. Ma, P. Fang and Z. Ling, Design, function, and implementation of China's first LIBS instrument (MarSCoDe) on the Zhurong Mars rover, *At. Spectrosc.*, 2021, **42**, 294–298, DOI: 10.46770/AS.2021.608.

86 N. Mezoued, C. Fabre, J. Cauzid, Y. Kim, M. Jatteau, N. Mezoued, C. Fabre, J. Cauzid, Y. Kim and M. Jatteau, Analysis of Minerals Using Handheld Laser-Induced Breakdown Spectroscopy Technology, *Data*, 2025, **10**, 10, DOI: 10.3390/DATA10030040.

87 M. A. Gondal, T. Hussain, Z. H. Yamani and A. H. Bakry, Study of hazardous metals in iron slag waste using laser induced breakdown spectroscopy, *J. Environ. Sci. Health, Part A: Toxic/Hazard. Subst. Environ. Eng.*, 2007, **42**, 767–775, DOI: 10.1080/10934520701304443.

88 M. Gaft, I. Sapir-Sofer, H. Modiano and R. Stana, Laser induced breakdown spectroscopy for bulk minerals online analyses, *Spectrochim. Acta, Part B*, 2007, **62**, 1496–1503, DOI: 10.1016/J.SAB.2007.10.041.

89 C. M. Ahamer, S. Eschlböck-Fuchs, P. J. Kolmhofer, R. Rössler, N. Huber and J. D. Pedarnig, Laser-induced breakdown spectroscopy of major and minor oxides in steel slags: influence of detection geometry and signal normalization, *Spectrochim. Acta, Part B*, 2016, **122**, 157–164, DOI: 10.1016/J.SAB.2016.06.008.

90 A. Ciucci, M. Corsi, V. Palleschi, S. Rastelli, A. Salvetti and E. Tognoni, New procedure for quantitative elemental analysis by laser-induced plasma spectroscopy, *Appl. Spectrosc.*, 1999, **53**, 960–964, DOI: 10.1366/0003702991947612.

91 E. Tognoni, G. Cristoforetti, S. Legnaioli and V. Palleschi, Calibration-Free Laser-Induced Breakdown Spectroscopy: State of the art, *Spectrochim. Acta, Part B*, 2010, **65**, 1–14, DOI: 10.1016/j.sab.2009.11.006.

92 F. Poggialini, B. Campanella, B. Cocciaro, G. Lorenzetti, V. Palleschi and S. Legnaioli, Catching up on calibration-free LIBS, *J. Anal. At. Spectrom.*, 2023, **38**, 1751–1771, DOI: 10.1039/D3JA00130J.

93 K. Rifai, L. Özcan, F. Doucet, N. Azami, L. Deshays, A. Lebbardi and F. Vidal, Rapid analysis of phosphate slurries and pressed pellets using laser-induced breakdown spectroscopy, *Spectrochim. Acta, Part B*, 2020, **163**, 105735, DOI: 10.1016/J.SAB.2019.105735.

94 H. Dong, L. Sun, L. Qi, H. Yu and P. Zeng, A lightweight convolutional neural network model for quantitative analysis of phosphate ore slurry based on laser-induced breakdown spectroscopy, *J. Anal. At. Spectrom.*, 2021, **36**, 2528–2535, DOI: 10.1039/d1ja00209k.

95 P. Zhang, L. Sun, L. Qi and H. Yu, On-line quantitative analysis of major elements in phosphate slurry using LIBS assisted by plasma information from orthogonal directions imaging, *Measurement*, 2024, **234**, 114827, DOI: 10.1016/J.MEASUREMENT.2024.114827.

96 A. N. Li, X. Zhang, X. Liu, Y. He, Y. Shan, H. Sun, W. Yi and R. Liu, Real time and high-precision online determination of main components in iron ore using spectral refinement

algorithm based LIBS, *Opt. Express*, 2023, **31**(23), 38728–38743, DOI: 10.1364/OE.505574.

97 S. Béchard and Y. Mouget, LIBS for the analysis of pharmaceutical materials, *Laser Induced Breakdown Spectroscopy (LIBS): Fundamentals and Applications*, 9780521852746, 2006, pp. 314–331, DOI: 10.1017/CBO9780511541261.009.

98 L. St-Onge, E. Kwong, M. Sabsabi and E. B. Vadas, Quantitative analysis of pharmaceutical products by laser-induced breakdown spectroscopy, *Spectrochim. Acta, Part B*, 2002, **57**, 1131–1140, DOI: 10.1016/S0584-8547(02)00062-9.

99 M. Gazmeh, M. Bahreini and S. H. Tavassoli, Discrimination of healthy and carious teeth using laser-induced breakdown spectroscopy and partial least square discriminant analysis, *Appl. Opt.*, 2015, **54**(1), 123–131, DOI: 10.1364/AO.54.000123.

100 A. Marín-Roldán, S. Manzoor, J. Krištof and P. Veis, Enlarged spectral range in Calibration Free – Laser Induced Breakdown Spectroscopy for the qualitative and quantitative analysis of a complex bone matrix, *Spectrochim. Acta, Part B*, 2019, **156**, 13–19, DOI: 10.1016/j.sab.2019.04.005.

101 Ş. Yalçin, D. R. R. Crosley, G. P. P. Smith and G. W. W. Faris, Influence of ambient conditions on the laser air spark, *Appl. Phys. B*, 1999, **68**, 121–130, DOI: 10.1007/s003400050596.

102 L. Pardini, S. Legnaioli, G. Lorenzetti, V. Palleschi, R. Gaudiuso, A. De Giacomo, D. M. Diaz Pace, F. Anabitarte Garcia, G. De Holanda Cavalcanti and C. Parigger, On the determination of plasma electron number density from Stark broadened hydrogen Balmer series lines in Laser-Induced Breakdown Spectroscopy experiments, *Spectrochim. Acta, Part B*, 2013, **88**, 98–103, DOI: 10.1016/j.sab.2013.05.030.

103 M. N. Khan, Q. Wang, B. S. Idrees, G. Teng, X. Cui and K. Wei, Discrimination of Melanoma Using Laser-Induced Breakdown Spectroscopy Conducted on Human Tissue Samples, *J. Spectrosc.*, 2020, **2020**, 8826243, DOI: 10.1155/2020/8826243.

104 V. Bali, N. Sharma, Y. Khajuria, Y. Lee, S. Kumar, P. K. Rai and V. K. Singh, Elemental Analysis of Fingernails for the Identification of Chronic Kidney Disease (CKD) by Laser-Induced Breakdown Spectroscopy (LIBS) and Energy Dispersive X-Ray Spectroscopy (EDS) with Partial Least Squares–Discriminant Analysis (PLS-DA), *Anal. Lett.*, 2025, **59**(10), 1752–1772, DOI: 10.1080/00032719.2025.2567596.

105 H. Xie, J. Huang, R. Wang, X. Ma, L. Xie, H. Zhang, J. Li and C. Liu, Elemental composition analysis of calcium-based urinary stones via laser-induced breakdown spectroscopy for enhanced clinical insights, *Sci. Rep.*, 2025, **15**(1), 33587, DOI: 10.1038/S41598-025-18749-6.